Eur. Phys. J. C (2023) 83:477
https://doi.org/10.1140/epjc/s10052-023-11576-x

THE EUROPEAN PHYSICAL JOURNAL C

Regular Article - Theoretical Physics

Covariant light-front approach for B_c decays into charmonium: implications on form factors and branching ratios

Zhi-Qing Zhang[a], **Zhi-Jie Sun, Yan-Chao Zhao, You-Ya Yang, Zi-Yu Zhang**

Institute of Theoretical Physics, School of Sciences, Henan University of Technology, Zhengzhou 450052, Henan, China

Received: 2 April 2023 / Accepted: 1 May 2023 / Published online: 7 June 2023

Abstract In this work, we investigate the form factors of B_c decays into J/Ψ, $\psi(2S, 3S)$, η_c, $\eta_c(2\,S, 3\,S)$, χ_{c0}, χ_{c1}, h_c, and $X(3872)$ mesons in the covariant light-front quark model (CLFQM). For the purpose of the branching ratio calculation, the form factors of $B_c \to D^{(*)}, D_s^{(*)}$ transitions are also included. In order to obtain the form factors for the physical transition processes, we need to extend these form factors from the space-like region to the time-like region. The q^2 dependence for each transition form factor is also plotted. Then, using the factorization method, we calculate the branching ratios of 80 B_c decay channels with a charmonium involved in each mode. Most of our predictions are comparable to the results given by other approaches. As to the decays with the radially excited-state S-wave charmonia involved, such as $\psi(2S, 3S)$ and $\eta_c(2S, 3S)$, two sets of parameters for their light-front wave functions, corresponding to scenario I (SI) and scenario II (SII), are adopted to calculate the branching ratios. By comparing with the future experimental data, one can discriminate which parameters are more favored.

1 Introduction

During the period from the 1970 s to 1980 s, the light-front quark model (LFQM) was developed [1,2] to deal with nonperturbative physical quantities such as decay constants, transition form factors, and so on. This relativistic quark model is based on a light-front formalism [3] and quantum chromodynamics (QCD) light-front quantization [4]. The LFQM can provide a relativistic treatment of the hadron momentum and full treatment of the quark spin by using the so-called Melosh rotation. At the same time, the light-front wave functions are independent of the hadron momentum and thus are manifestly Lorentz-invariant. Equipped with these advantages, the LFQM becomes a convenient approach and has been employed to calculate decay constants and form factors [5–9]. While under the LFQM, the constituent quark and antiquark in a bound state are required to be on their mass shells, which makes degrees of freedom of light-front momentum become three and the Lorentz covariance of the matrix elements to be lost. The usual practice is only taking the plus component ($\mu = +$) of the current matrix elements, which will miss the zero-mode contribution. However, lacking the zero-mode contributions sometimes affects the calculation accuracy. Unfortunately, such a conventional LFQM approach with a defect is powerless to calculate the zero-mode contribution. At the end of the twentieth century, Jaus put forward the covariant light-front quark model (CLFQM) [10]. The previous LFQM is usually called the standard light-front quark model (SLFQM) [10]. The CLFQM is more convincing than the SLFQM. In the CLFQM approach [10], when evaluating the light-front matrix element from the momentum loop integral by a light-front decomposition to the internal momentum and carrying out the integration over the minus component ($p^- = p^0 - p^3$) by means of contour methods, one will encounter additional spurious contributions proportional to the light-like vector $\omega^\mu = (0, 2, 0_\perp)$, which violates the covariance. While this spurious contribution is just canceled by the zero-mode contribution, at the same time the covariance of the current matrix elements is restored, and all the problems can be resolved. Since the popular CLFQM was proposed, it has been widely used to study the form factors and the decay constants of the ground-state S-wave and low-lying P-wave mesons, and is further applied to phenomenological studies about B_c decays [11–15]. Certainly, there still exist some discussions about the self-consistency of the CLFQM, for example, the decay constant of the vector meson, which is different as a result of extracting from different polarization (longitudinal and transverse) states [16–19].

[a] e-mail: zhangzhiqing@haut.edu.cn (corresponding author)

B_c meson decays have received extensive attention because of its unique structure in the Standard Model. The B_c meson is the only heavy meson composed of two heavy quarks with different flavors (b and c), which cannot annihilate into gluons (photon) via strong (electromagnetic) interaction. Decays of the B_c meson occur only via weak interaction, which includes three types at the quark level, the $b \to c(u)$, $c \to s(d)$ transitions, and the weak annihilations. Although the phase space of the c quark decays is much smaller than that of the b quark decays, the Cabibbo–Kobayashi–Maskawa (CKM) matrix elements are greatly in favor of the c quark decays (i.e., $|V_{cs}| \gg |V_{cb}|, |V_{cd}| \gg |V_{ub}|$), which provide about 70% of the B_c decay width, while the b quark decays and the weak annihilations only amount to about 20% and 10%, respectively [20]. On the experimental side, since the B_c meson was first discovered by the Collider Detector at Fermilab (CDF) collaboration via the decay of $B_c \to J/\Psi l\nu$ in 1.8-TeV $p\bar{p}$ collisions at the Fermilab Tevatron, many B_c decay channels have been observed by the Large Hadron Collider beauty (LHCb) collaboration, such as $B_c^+ \to J/\Psi\pi^+\pi^-\pi^+$ [21], $B_c^+ \to J/\Psi\pi^+$ [22], $B_c^+ \to J/\Psi K^+$ [23], $B_c^+ \to J/\Psi D_s^{(*)+}$ [24], $B_c^+ \to J/\Psi K^+K^-\pi^+$ [25], and $B_c^+ \to B_s^0\pi^+$ [26]. The inclusive production cross section of the B_c meson at the LHC is estimated to be at a level of $1\mu b$ for $\sqrt{14}$ TeV. This means that around $\mathcal{O}(10^9)$ B_c events with a luminosity of $1 fb^{-1}$ can be provided [27], which are sufficient for studying the B_c meson decays. On the theoretical side, many theoretical methods have been used to study the B_c meson decays to charmonium states, such as the perturbation QCD (PQCD) approach [28,29], the generalized factorization (GF) approach [30], the QCD factorization (QCDF) approach [31], the QCD sum rule (QCDSR) approach [32], the Bethe–Salpter equation approach [33], the relativistic quark model (RQM) [34,35], and nonrelativistic QCD approach(NRQCD) [36].

The development of the theoretical and experimental aspects of the B_c meson physics motivates us to investigate the B_c weak decays with a charmonium involved in each mode. In Sect. 2, we recapitulate the CLFQM, including the definitions of the decay constants and the relevant formulae of B_c to charmonium or charmed meson transition form factors. In Sect. 3, after determining the shape parameters β' using the corresponding decay constants, we provide the numerical results of B_c transition form factors and their q^2 dependence. Then, using the transition form factors, we calculate the branching ratios of B_c decays with a charmonium meson involved in each mode. In addition, detailed data analysis and discussion, including a comparison with the other model calculations, are carried out. The conclusions are presented in the final part.

Table 1 Feynman rules for the vertices $i\Gamma'_M$ of the incoming meson–quark–antiquark, where p'_1 and p_2 are the quark and antiquark momenta, respectively

$M\,(^{2S+1}L_J)$	$i\Gamma'_M$
Pseudoscalar $(^1S_0)$	$H'_P\gamma_5$
Vector $(^3S_1)$	$iH'_V\left[\gamma_\mu - \frac{1}{W'_V}(p'_1 - p_2)_\mu\right]$
Scalar $(^3P_0)$	$-iH'_S$
Axial $(^3P_1)$	$-iH'_{3_A}\left[\gamma_\mu + \frac{1}{W'_{3_A}}(p'_1 - p_2)_\mu\right]\gamma_5$
Axial $(^1P_1)$	$-iH'_{1_A}\left[\frac{1}{W'_{1_A}}(p'_1 - p_2)_\mu\right]\gamma_5$

2 Formalism

2.1 Covariant light-front quark model

Under the covariant light-front quark model, the light-front coordinates of a momentum p are used, $p = (p^-, p^+, p_\perp)$, with $p^\pm = p^0 \pm p_z$, $and p^2 = p^+p^- - p_\perp^2$. The Feynman diagrams for B_c meson decay and transition amplitudes are shown in Fig. 1. The incoming (outgoing) meson has mass $M'(M'')$ with momentum $P' = p'_1 + p_2 (P'' = p''_1 + p_2)$, where $p_1^{\prime(\prime\prime)}$ and p_2 are the momenta of the quark and antiquark inside the incoming (outgoing) meson with mass $m_1^{\prime(\prime\prime)}$ and m_2, respectively. Here, we use the same notation as those in Refs. [10,11] and $M' = m_{B_c}$ for B_c meson decays. These momenta can be expressed in terms of the internal variables $(x_i, p'_\perp)$ as

$$p'^+_{1,2} = x_{1,2}P'^+, \quad p'_{1,2\perp} = x_{1,2}P'_\perp \pm p'_\perp \tag{1}$$

with $x_1 + x_2 = 1$. Using these internal variables, we can define some quantities for the incoming meson which will be used in the following calculations:

$$\begin{aligned} M_0'^2 &= \left(e'_1 + e_2\right)^2 = \frac{p_\perp'^2 + m_1'^2}{x_1} + \frac{p_\perp^2 + m_2^2}{x_2}, \\ \widetilde{M}'_0 &= \sqrt{M_0'^2 - \left(m'_1 - m_2\right)^2}, \\ e_i^{(\prime)} &= \sqrt{m_i^{(\prime)2} + p_\perp'^2 + p_z'^2}, \\ p'_z &= \frac{x_2 M'_0}{2} - \frac{m_2^2 + p_\perp'^2}{2x_2 M'_0}, \end{aligned} \tag{2}$$

where M'_0 is the kinetic invariant mass of the incoming meson and can be expressed as the energies of the quark and the antiquark $e_i^{(\prime)}$. It is similar to the case of the outgoing meson.

To calculate the amplitudes for the transition form factors, we need the Feynman rules for the meson–quark–antiquark vertices $(i\Gamma'_M(M = P, V, A, S))$, which are listed in Table 1. It is noted that for the outgoing meson, we should use $i(\gamma_0\Gamma_M'^\dagger\gamma_0)$ for the relevant vertices. The $B_c \to M$ $(M$

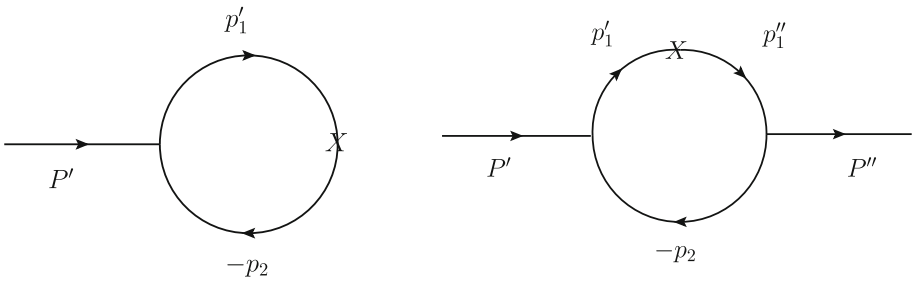

Fig. 1 Feynman diagram for B_c decay (left) and transition (right) amplitudes, where $P'^{(\prime\prime)}$ is the incoming (outgoing) meson momentum, $p_1^{\prime(\prime\prime)}$ is the quark momentum, p_2 is the antiquark momentum, and X denotes the vector or axial vector transition vertex

denotes a pseudoscalar (P), a vector (V), an axial vector (A), or a scalar (S) meson) form factors induced by vector and axial-vector currents are defined as

$$\langle P(P'')|V_\mu|B_c(P')\rangle = f_+(q^2)P_\mu + f_-(q^2)q_\mu, \tag{3}$$

$$\langle V(P'',\varepsilon)|V_\mu|B_c(P')\rangle = \epsilon_{\mu\nu\alpha\beta}\varepsilon^{*\nu}P^\alpha q^\beta g(q^2), \tag{4}$$

$$\langle V(P'',\varepsilon)|A_\mu|B_c(P')\rangle = -i\left\{\varepsilon_\mu^* f(q^2) + \varepsilon^*\cdot P\left[P_\mu a_+(q^2) + q_\mu a_-(q^2)\right]\right\}, \tag{5}$$

$$\left\langle {}^1A(P'',\varepsilon)|A_\mu|B_c(P')\right\rangle = -q\,{}^1A(q^2)\epsilon_{\mu\nu\alpha\beta}\varepsilon^{*\nu}P^\alpha q^\beta, \tag{6}$$

$$\left\langle {}^1A(P'',\varepsilon)|V_\mu|B_c(P')\right\rangle = i\left\{l\,{}^1A(q^2)\varepsilon_\mu^* + \varepsilon^*\cdot P\left[P_\mu c_+{}^1A(q^2) + q_\mu c_-{}^1A(q^2)\right]\right\}, \tag{7}$$

$$\left\langle {}^3A(P'',\varepsilon)|A_\mu|B_c(P')\right\rangle = -q\,{}^3A(q^2)\epsilon_{\mu\nu\alpha\beta}\varepsilon^{*\nu}P^\alpha q^\beta, \tag{8}$$

$$\left\langle {}^3A(P'',\varepsilon)|V_\mu|B_c(P')\right\rangle = i\left\{l\,{}^3A(q^2)\varepsilon_\mu^* + \varepsilon^*\cdot P\left[P_\mu c_+{}^3A(q^2) + q_\mu c_-{}^3A(q^2)\right]\right\}, \tag{9}$$

$$\langle S(P'')|A_\mu|B_c(P')\rangle = i\left[u_+(q^2)P_\mu + u_-(q^2)q_\mu\right]. \tag{10}$$

In calculations, the Bauer–Stech–Wirbel (BSW) [37] form factors for the $B_c \to M$ transition are more frequently used and defined by

$$\langle P(P'')|V_\mu|B_c(P')\rangle = \left(P_\mu - \frac{m_{B_c}^2 - m_P^2}{q^2}q_\mu\right)F_1^{B_cP}(q^2) + \frac{m_{B_c}^2 - m_P^2}{q^2}q_\mu F_0^{B_cP}(q^2), \tag{11}$$

$$\langle V(P'',\varepsilon^{\mu*})|V_\mu|B_c(P')\rangle = -\frac{1}{m_{B_c}+m_V}\epsilon_{\mu\nu\alpha\beta}\varepsilon^{*\nu}P^\alpha q^\beta V^{B_cV}(q^2), \tag{12}$$

$$\langle V(P'',\varepsilon^{\mu*})|A_\mu|B_c(P')\rangle = i\left\{(m_{B_c}+m_V)\varepsilon_\mu^* A_1^{B_cV}(q^2) - \frac{\varepsilon^*\cdot P}{m_{B_c}+m_V}P_\mu A_2^{B_cV}(q^2) - 2m_V\frac{\varepsilon^*\cdot P}{q^2}q_\mu\left[A_3^{B_cV}(q^2) - A_0^{B_cV}(q^2)\right]\right\}, \tag{13}$$

$$\langle A(P'',\varepsilon^{\mu*})|V_\mu|B_c(P')\rangle = -i\left\{(m_{B_c}-m_A)\varepsilon_\mu^* V_1^{B_cA}(q^2) - \frac{\varepsilon^*\cdot P}{m_{B_c}-m_A}P_\mu V_2^{B_cA}(q^2) - 2m_A\frac{\varepsilon^*\cdot P}{q^2}q_\mu\left[V_3^{B_cA}(q^2) - V_0^{B_cA}(q^2)\right]\right\}, \tag{14}$$

$$\langle A(P'',\varepsilon^{\mu*})|A_\mu|B_c(P')\rangle = -\frac{1}{m_{B_c}-m_A}\epsilon_{\mu\nu\alpha\beta}\varepsilon^{*\nu}P^\alpha q^\beta A^{B_cA}(q^2), \tag{15}$$

$$\langle S(P'')|A_\mu|B_c(P')\rangle = \left(P_\mu - \frac{m_{B_c}^2 - m_S^2}{q^2}q_\mu\right)F_1^{B_cS}(q^2) + \frac{m_{B_c}^2 - m_S^2}{q^2}q_\mu F_0^{B_cS}(q^2), \tag{16}$$

where $P = P' + P'', q = P' - P''$, and the convention $\epsilon_{0123} = 1$ is adopted.

To smear the singularity at $q^2 = 0$ in Eqs. (13) and (14), the relations $V_3^{B_cA}(0) = V_0^{B_cA}(0)$, $A_3^{B_cV}(0) = A_0^{B_cV}(0)$ are required, and

$$V_3^{B_cA}(q^2) = \frac{m_{B_c}-m_A}{2m_A}V_1^{B_cA}(q^2) - \frac{m_{B_c}+m_A}{2m_A}V_2^{B_cA}(q^2), \tag{17}$$

$$A_3^{B_cV}(q^2) = \frac{m_{B_c}+m_V}{2m_V}A_1^{B_cV}(q^2) - \frac{m_{B_c}-m_V}{2m_V}A_2^{B_cV}(q^2). \tag{18}$$

These two kinds of form factors are related to each other via

$$F_1^{B_cP}(q^2) = f_+(q^2),\ F_0^{B_cP}(q^2) = f_+(q^2) + \frac{q^2}{q\cdot P}f_-(q^2), \tag{19}$$

$$V^{B_cV}(q^2) = -(m_{B_c}+m_V)g(q^2),\ A_1^{B_cV}(q^2) = -\frac{f(q^2)}{m_{B_c}+m_V}, \tag{20}$$

$$A_2^{B_cV}(q^2) = (m_{B_c}+m_V)a_+(q^2),\ A_3^{B_cV}(q^2) - A_0^{B_cV}(q^2) = \frac{q^2}{2m_V}a_-(q^2), \tag{21}$$

$$A^{B_cA}(q^2) = -(m_{B_c}-m_A)q(q^2),\ V_1^{B_cA}(q^2) = -\frac{l(q^2)}{m_{B_c}-m_A}, \tag{22}$$

$$V_2^{B_cA}(q^2) = (m_{B_c} - m_A)c_+(q^2),\ V_3^{B_cA}(q^2) - V_0^{B_cA}(q^2) = \frac{q^2}{2m_A}c_-(q^2), \tag{23}$$

$$F_1^{B_cS}(q^2) = -u_+(q^2),\ F_0^{B_cS}(q^2) = -u_+(q^2) - \frac{q^2}{q\cdot P}u_-(q^2). \tag{24}$$

2.2 Wave functions and decay constants

In order to calculate the form factors, we need to specify the light-front wave functions. In principle, one can obtain them by solving the relativistic Schrödinger equation. But it is difficult to obtain the exact solution in many cases. Therefore, phenomenological wave functions are usually employed to describe the hadronic structure. In the present work, we shall use the phenomenological Gaussian-type wave functions

$$\varphi' = \varphi'\left(x_2, p'_\perp\right) = 4\left(\frac{\pi}{\beta'^2}\right)^{\frac{3}{4}}\sqrt{\frac{\mathrm{d}p'_z}{\mathrm{d}x_2}}\exp\left(-\frac{p_z'^2 + p_\perp'^2}{2\beta'^2}\right),$$
$$\varphi'_p = \varphi'_p\left(x_2, p'_\perp\right) = \sqrt{\frac{2}{\beta'^2}}\varphi',\quad \frac{\mathrm{d}p'_z}{\mathrm{d}x_2} = \frac{e'_1 e_2}{x_1 x_2 M'_0}, \tag{25}$$

where the parameter β' describes the momentum distribution and is approximately of order Λ_{QCD}. It is usually determined by the decay constants through the analytic expressions in the conventional light-front approach, which are given as follows [10,11]:

$$f_P = \frac{N_c}{16\pi^3}\int \mathrm{d}x_2 d^2p'_\perp \frac{h'_P}{x_1x_2(M'^2 - M_0'^2)}4\left(m'_1x_2 + m_2x_1\right), \tag{26}$$

$$f_V = \frac{N_c}{4\pi^3 M'}\int \mathrm{d}x_2 d^2p'_\perp \frac{h'_V}{x_1x_2\left(M'^2 - M_0'^2\right)} \times\left[x_1M_0'^2 - m'_1\left(m'_1 - m_2\right) - p_\perp'^2 + \frac{m'_1 + m_2}{w'_V}p_\perp'^2\right], \tag{27}$$

$$f_{^3A} = -\frac{N_c}{4\pi^3 M'}\int \mathrm{d}x_2 d^2p'_\perp \frac{h'_{^3A}}{x_1x_2\left(M'^2 - M_0'^2\right)} \times\left[x_1M_0'^2 - m'_1\left(m'_1 + m_2\right) - p_\perp'^2 - \frac{m'_1 - m_2}{w'_{^3A}}p_\perp'^2\right], \tag{28}$$

$$f_{^1A} = \frac{N_c}{4\pi^3 M'}\int \mathrm{d}x_2 d^2p'_\perp \frac{h'_{^3A}}{x_1x_2\left(M'^2 - M_0'^2\right)}\left(\frac{m'_1 - m_2}{w'_{^1A}}p_\perp'^2\right), \tag{29}$$

$$f_S = \frac{N_c}{16\pi^3}\int \mathrm{d}x_2 d^2p'_\perp \frac{h'_S}{x_1x_2\left(M'^2 - M_0'^2\right)}4\left(m'_1x_2 - m_2x_1\right), \tag{30}$$

where m'_1 and m_2 are the constituent quarks of meson $M(M = P, V,\ ^3A,\ ^1A, S)$. By the way, a tensor meson ($^3P_2$ state) cannot be produced through $(V \pm A)$ or tensor current, so we should not define its decay constant. The explicit forms of h'_M are given by [11]

$$h'_P = h'_V = \left(M'^2 - M_0'^2\right)\sqrt{\frac{x_1x_2}{N_c}}\frac{1}{\sqrt{2}\widetilde{M}'_0}\varphi', \tag{31}$$

$$h'_S = \sqrt{\frac{2}{3}}h'_{^3A} = \left(M'^2 - M_0'^2\right)\sqrt{\frac{x_1x_2}{N_c}}\frac{1}{\sqrt{2}\widetilde{M}'_0}\frac{\widetilde{M}_0'^2}{2\sqrt{3}M'_0}\varphi'_p, \tag{32}$$

$$h'_{^1A} = \left(M^{2\prime} - M_0'^2\right)\sqrt{\frac{x_1x_2}{N_c}}\frac{1}{\sqrt{2}\widetilde{M}'_0}\varphi'_p. \tag{33}$$

It is easy to see that the decay constants of the scalar meson and ^1A type of axial meson are zero for $m'_1 = m_2$, which satisfies the $SU(N)$ flavor constraint. The other nontrivial decay constants can be obtained through the experimental results for the purely leptonic decays or the lattice QCD calculations. The constituent quark masses used in the calculations will be listed in the next section.

2.3 Form factors

One important difference between the conventional light-front quark approach and the covariant one lies in the treatment of the constituent quarks. In the conventional light-front framework, the constituent quarks are required to be on their mass shells, and the physical quantities, such as decay constant and form factor, can be extracted from the plus component of the corresponding current matrix elements. However, this framework misses the zero-mode contributions and renders the matrix elements non-covariant. In order to resolve this problem, the covariant light-front approach was proposed by Jaus [10], which provides a systematical way to deal with the zero-mode contributions by including the so-called Z-diagram contributions. Then physical quantities can be calculated in terms of Feynman momentum loop integrals in a manifestly covariant way. As a result, the constituent quarks of the meson will be off-shell. For the general $B_c \to P$ transition, the decay amplitude for the lowest order is

$$\mathcal{B}_\mu^{B_cP} = -i^3\frac{N_c}{(2\pi)^4}\int d^4p'_1 \frac{H'_{B_c}\left(H''_P\right)}{N'_1N''_1N_2}S_\mu^{B_cP}, \tag{34}$$

where $N_1^{\prime(\prime\prime)} = p_1^{\prime(\prime\prime)2} - m_1^{\prime(\prime\prime)2}$, $N_2 = p_2^2 - m_2^2$ arise from the quark propagators, and the trace $S_\mu^{B_cP}$ can be directly obtained by using the Lorentz contraction,

$$\begin{aligned} S_\mu^{B_cP} &= \mathrm{Tr}\left[\gamma_5\left(\not{p}''_1 + m''_1\right)\gamma_\mu\left(\not{p}'_1 + m'_1\right)\gamma_5(-\not{p}_2 + m_2)\right] \\ &= 2p'_{1\mu}\Big[M'^2 + M''^2 - q^2 - 2N_2 - \left(m'_1 - m_2\right)^2 \\ &\quad - \left(m''_1 - m_2\right)^2 + \left(m'_1 - m''_1\right)^2\Big] \\ &\quad + q_\mu\Big[q^2 - 2M'^2 + N'_1 - N''_1 + 2N_2 + 2\left(m'_1 - m_2\right)^2 \end{aligned}$$

$$-\left(m_1'-m_1''\right)^2\Big]$$
$$+P_\mu\left[q^2-N_1'-N_1''-\left(m_1'-m_1''\right)^2\right]. \tag{35}$$

In practice, we use the light-front decomposition of the Feynman loop momentum and integrate out the minus component through the contour method. If the covariant vertex functions are not singular when performing integration, the transition amplitudes will pick up the singularities in the antiquark propagators. The integration then leads to

$$\begin{aligned} N_1'^{(\prime)} &\to \hat{N}_1'^{(\prime)} = x_1\left(M'^{(\prime)2}-M_0'^{(\prime)2}\right),\\ H_M'^{(\prime)} &\to h_M'^{(\prime)}\\ W_M'' &\to w_M''\\ \int\frac{d^4p_1'}{N_1'N_1''N_2}H'_{B_c}H''_M S^{B_cM} &\to -i\pi\int\frac{\mathrm{d}x_2d^2p_\perp'}{x_2\hat{N}_1'\hat{N}_1''}h'_{B_c}h''_M\hat{S}^{B_cM}, \end{aligned} \tag{36}$$

where

$$M_0''^2=\frac{p_\perp''^2+m_1''^2}{x_1}+\frac{p_\perp''^2+m_2^2}{x_2}, \tag{37}$$

with $p_\perp''=p_\perp'-x_2q_\perp$, and M in the subscript and superscript denotes a pseudoscalar (P), a vector (V), an axial vector (A), or a scalar (S) meson. The explicit forms of $h_M'^{(\prime)}$ have been given in Eqs. (31)–(33). For the $B_c\to V$, A transitions, the $\omega_M''(M=V,A)$ in the corresponding vertex operators listed in Table 1 are given as

$$w_V''=M_0''+m_1''+m_2,\quad w_{3A}''=\frac{\widetilde{M}_0''^2}{m_1''-m_2},\quad w_{1A}''=2, \tag{38}$$

where $\widetilde{M}_0''=\sqrt{M_0''^2-\left(m_1''-m_2\right)^2}$.

After performing the integration with the contour method, we will be confronted with additional spurious contributions proportional to the light-like four-vector $\tilde{\omega}=(0,2,\mathbf{0}_\perp)$. These undesired spurious contributions can be eliminated by inclusion of the zero-mode contributions, which amount to performing the p^- integration in a proper way. The specific rules under the p^- integration have been derived in Refs. [10,11], and the relevant ones are collected in the Appendix.

Using Eqs. (35)–(37) and taking the integration rules given in Refs. [10,11], we obtain the $B_c\to P$ form factors,

$$\begin{aligned} f_+\left(q^2\right) &= \frac{N_c}{16\pi^3}\int\mathrm{d}x_2d^2p_\perp'\frac{h'_{B_c}h''_P}{x_2\hat{N}_1'\hat{N}_1''}\Big[x_1\left(M_0'^2+M_0''^2\right)+x_2q^2\\ &\quad -x_2\left(m_1'-m_1''\right)^2-x_1\left(m_1'-m_2\right)^2-x_1\left(m_1''-m_2\right)^2\Big], \end{aligned} \tag{39}$$

$$\begin{aligned} f_-\left(q^2\right) &= \frac{N_c}{16\pi^3}\int\mathrm{d}x_2d^2p_\perp'\frac{2h'_{B_c}h''_P}{x_2\hat{N}_1'\hat{N}_1''}\\ &\quad\times\Big\{-x_1x_2M'^2-p_\perp'^2-m_1'm_2+\left(m_1''-m_2\right)\\ &\quad\times\left(x_2m_1'+x_1m_2\right)\\ &\quad+2\frac{q\cdot P}{q^2}\left(p_\perp'^2+2\frac{\left(p_\perp'\cdot q_\perp\right)^2}{q^2}\right)+2\frac{\left(p_\perp'\cdot q_\perp\right)^2}{q^2}-\frac{p_\perp'\cdot q_\perp}{q^2}\\ &\quad\times\Big[M''^2-x_2\left(q^2+q\cdot P\right)\\ &\quad-\left(x_2-x_1\right)M'^2+2x_1M_0'^2-2\left(m_1'-m_2\right)\left(m_1'+m_1''\right)\Big]\Big\}. \end{aligned} \tag{40}$$

It is similar for the $B_c\to V$ transition amplitudes, which are given by [11]

$$\mathcal{B}_\mu^{B_cV}=-i^3\frac{N_c}{(2\pi)^4}\int d^4p_1'\frac{H'_{B_c}\left(iH_V''\right)}{N_1'N_1''N_2}S_{\mu\nu}^{B_cV}\varepsilon^{*\nu}, \tag{41}$$

where

$$\begin{aligned} S_{\mu\nu}^{B_cV} &= \left(S_V^{B_cV}-S_A^{B_cV}\right)_{\mu\nu}\\ &= \mathrm{Tr}\Big[\left(\gamma_\nu-\frac{1}{W_V''}\left(p_1''-p_2\right)_\nu\right)\\ &\quad\times\left(p_1''+m_1''\right)\left(\gamma_\mu-\gamma_\mu\gamma_5\right)\left(\not{p}_1'+m_1'\right)\gamma_5\left(-\not{p}_2+m_2\right)\Big]\\ &= -2i\epsilon_{\mu\nu\alpha\beta}\Big\{p_1'^\alpha P^\beta\left(m_1''-m_1'\right)\\ &\quad+p_1''^\alpha q^\beta\left(m_1''+m_1'-2m_2\right)+q^\alpha P^\beta m_1'\Big\}\\ &\quad+\frac{1}{W_V''}\left(4p'_{1\nu}-3q_\nu-P_\nu\right)i\epsilon_{\mu\alpha\beta\rho}p_1'^\alpha q^\beta P^\rho\\ &\quad+2g_{\mu\nu}\Big\{m_2\left(q^2-N_1'-N_1''-m_1'^2-m_1''^2\right)\\ &\quad-m_1'\left(M''^2-N_1''-N_2-m_1''^2-m_2^2\right)\\ &\quad-m_1''\left(M'^2-N_1'-N_2-m_1'^2-m_2^2\right)-2m_1'm_1''m_2\Big\}\\ &\quad+8p'_{1\mu}p'_{1\nu}\left(m_2-m_1'\right)-2\left(P_\mu q_\nu+q_\mu P_\nu+2q_\mu q_\nu\right)m_1'\\ &\quad+2p'_{1\mu}P_\nu\left(m_1'-m_1''\right)\\ &\quad+2p'_{1\mu}q_\nu\left(3m_1'-m_1''-2m_2\right)+2P_\mu p'_{1\nu}\left(m_1'+m_1''\right)\\ &\quad+2q_\mu p'_{1\nu}\left(3m_1'+m_1''-2m_2\right)\\ &\quad+\Big\{2p'_{1\mu}\left[M'^2+M''^2-q^2-2N_2+2\left(m_1'-m_2\right)\left(m_1''+m_2\right)\right]\\ &\quad+q_\mu\Big[q^2-2M'^2+N_1'-N_1''+2N_2\\ &\qquad-\left(m_1+m_1''\right)^2+2\left(m_1'-m_2\right)^2\Big]\\ &\quad+P_\mu\left[q^2-N_1'-N_1''-\left(m_1'+m_1''\right)^2\right]\Big\}\\ &\quad\times\frac{1}{2W_V''}\left(4p'_{1\nu}-3q_\nu-P_\nu\right). \end{aligned} \tag{42}$$

From the above equation, we can get the expressions for $B_c\to V$ form factors defined in Eqs. (4) and (5) [11]

$$\begin{aligned} g(q^2) &= -\frac{N_c}{16\pi^3}\int\mathrm{d}x_2d^2p_\perp'\frac{2h'_{B_c}h''_V}{x_2\hat{N}_1'\hat{N}_1''}\\ &\quad\times\Big\{x_2m_1'+x_1m_2+\left(m_1'-m_1''\right)\frac{p_\perp'\cdot q_\perp}{q^2} \end{aligned}$$

$$+\frac{2}{w_V''}\left[p_\perp'^2+\frac{\left(p_\perp'\cdot q_\perp\right)^2}{q^2}\right]\Bigg\}, \tag{43}$$

$$\begin{aligned} f(q^2) = {} & \frac{N_c}{16\pi^3}\int \mathrm{d}x_2 d^2p_\perp' \frac{h'_{B_c}h''_V}{x_2\hat{N}_1'\hat{N}_1''} \\ & \times\Big\{2x_1\left(m_2-m_1'\right)\left(M_0'^2+M_0''^2\right) \\ & -4x_1m_1''M_0'^2+2x_2m_1'q\cdot P \\ & +2m_2q^2-2x_1m_2\left(M'^2+M''^2\right) \\ & +2\left(m_1'-m_2\right) \\ & \left(m_1'+m_1''\right)^2+8\left(m_1'-m_2\right) \\ & \times\left[p_\perp'^2+\frac{\left(p_\perp'\cdot q_\perp\right)^2}{q^2}\right] \\ & +2\left(m_1'+m_1''\right)\left(q^2+q\cdot P\right)\frac{p_\perp'\cdot q_\perp}{q^2} \\ & -4\frac{q^2p_\perp'^2+\left(p_\perp'\cdot q_\perp\right)^2}{q^2w_V''} \\ & \times\left[2x_1\left(M'^2+M_0'^2\right)-q^2-q\cdot P-2\left(q^2+q\cdot P\right)\right. \\ & \left.\times\frac{p_\perp'\cdot q_\perp}{q^2}\right. \\ & \left.-2\left(m_1'-m_1''\right)\left(m_1'-m_2\right)\right]\Big\}, \end{aligned} \tag{44}$$

$$\begin{aligned} a_+(q^2) = {} & \frac{N_c}{16\pi^3}\int \mathrm{d}x_2 d^2p_\perp' \frac{2h'_{B_c}h''_V}{x_2\hat{N}_1'\hat{N}_1''} \\ & \times\Big\{\left(x_1-x_2\right)\left(x_2m_1'+x_1m_2\right) \\ & -\left[2x_1m_2+m_1''+\left(x_2-x_1\right)m_1'\right] \\ & \times\frac{p_\perp'\cdot q_\perp}{q^2}-2\frac{x_2q^2+p_\perp'\cdot q_\perp}{x_2q^2w_V''} \\ & \times\left[p_\perp'\cdot p_\perp''+\left(x_1m_2+x_2m_1'\right)\right. \\ & \left.\times\left(x_1m_2-x_2m_1''\right)\right]\Big\}, \end{aligned} \tag{45}$$

$$\begin{aligned} a_-(q^2) = {} & \frac{N_c}{16\pi^3}\int \mathrm{d}x_2 d^2p_\perp' \frac{h'_{B_c}h''_V}{x_2\hat{N}_1'\hat{N}_1''} \\ & \times\left\{2\left(2x_1-3\right)\left(x_2m_1'+x_1m_2\right)-8\left(m_1'-m_2\right)\right. \\ & \times\left[\frac{p_\perp'^2}{q^2}+2\frac{\left(p_\perp'\cdot q_\perp\right)^2}{q^4}\right] \\ & -\left[\left(14-12x_1\right)m_1'-2m_1''-\left(8-12x_1\right)m_2\right]\frac{p_\perp'\cdot q_\perp}{q^2} \\ & +\frac{4}{w_V''}\left(\left[M'^2+M''^2-q^2+2\left(m_1'-m_2\right)\left(m_1''+m_2\right)\right]\right. \\ & \times\left(A_3^{(2)}+A_4^{(2)}-A_2^{(1)}\right) \\ & +Z_2\left(3A_2^{(1)}-2A_4^{(2)}-1\right)+\frac{1}{2} \\ & \left[x_1\left(q^2+q\cdot P\right)-2M'^2-2p_\perp'\cdot q_\perp-2m_1'\left(m_1''+m_2\right)\right. \\ & \left.\left.-2m_2\left(m_1'-m_2\right)\right]\left(A_1^{(1)}+A_2^{(1)}-1\right)q\cdot P \\ & \left.\left.\left[\frac{p_\perp'^2}{q^2}+\frac{\left(p_\perp'\cdot q_\perp\right)^2}{q^4}\right]\left(4A_2^{(1)}-3\right)\right)\right\}, \end{aligned} \tag{46}$$

where the functions $A_1^{(1)}$, $A_2^{(1)}$, $A_3^{(2)}$, $A_4^{(2)}$ and Z_2 are listed in the Appendix, and the physical form factors $V^{B_cV}(q^2)$, $A_0^{B_cV}(q^2)$, $A_1^{B_cV}(q^2)$, *and* $A_2^{B_cV}(q^2)$ can be related to the above formulae through Eqs. (20) and (21).

The extension to $B_c\to A$ transitions is straightforward, and their form factors have similar expressions as those in the $B_c\to V$ transitions case. The $B_c\to {}^3A$, ${}^1A$ transition amplitudes are defined as [11]

$$\mathcal{B}_\mu^{B_c\,{}^1A} = -i^3\frac{N_c}{(2\pi)^4}\int d^4p_1'\frac{H'_{B_c}H''_{1_A}}{N_1'N_1''N_2}S_{\mu\nu}^{B_c\,{}^1A}\varepsilon''^{*\nu}, \tag{47}$$

$$\mathcal{B}_\mu^{B_c\,{}^3A} = -i^3\frac{N_c}{(2\pi)^4}\int d^4p_1'\frac{H'_{B_c}H''_{3_A}}{N_1'N_1''N_2}S_{\mu\nu}^{B_c\,{}^3A}\varepsilon''^{*\nu}, \tag{48}$$

where the traces $S_{\mu\nu}^{B_c\,{}^iA}(i=1,3)$

$$\begin{aligned} S_{\mu\nu}^{B_c\,{}^3A} = {} & \left(S_V^{B_c\,{}^3A}-S_A^{B_c\,{}^3A}\right)_{\mu\nu} \\ = {} & \mathrm{Tr}\left[\left(\gamma_\nu-\frac{1}{W''_{{}^3A}}\left(p_1''-p_2\right)_\nu\right)\right. \\ & \times\gamma_5\left(\not{p}_1''+m_1''\right)\left(\gamma_\mu-\gamma_\mu\gamma_5\right) \\ & \left.\times\left(\not{p}_1'+m_1'\right)\gamma_5\left(-\not{p}_2+m_2\right)\right] \\ = {} & \mathrm{Tr}\left[\left(\gamma_\nu-\frac{1}{W''_{{}^3A}}\left(p_1''-p_2\right)_\nu\right)\right. \\ & \times\left(\not{p}_1''-m_1''\right)\left(\gamma_\mu\gamma_5-\gamma_\mu\right) \\ & \left.\times\left(\not{p}_1'+m_1'\right)\gamma_5\left(-\not{p}_2+m_2\right)\right], \end{aligned} \tag{49}$$

$$\begin{aligned} S_{\mu\nu}^{B_c\,{}^1A} = {} & \left(S_V^{B_c\,{}^1A}-S_A^{B_c\,{}^1A}\right)_{\mu\nu} \\ = {} & \mathrm{Tr}\left[\left(-\frac{1}{W''_{{}^1A}}\left(p_1''-p_2\right)_\nu\right)\gamma_5\left(\not{p}_1''+m_1''\right)\right. \\ & \left.\times\left(\gamma_\mu-\gamma_\mu\gamma_5\right)\left(\not{p}_1'+m_1'\right)\gamma_5\left(-\not{p}_2+m_2\right)\right] \\ = {} & \mathrm{Tr}\left[\left(-\frac{1}{W''_{{}^1A}}\left(p_1''-p_2\right)_\nu\right)\left(\not{p}_1''-m_1''\right)\left(\gamma_\mu\gamma_5\right.\right. \\ & \left.\left.-\gamma_\mu\right)\left(\not{p}_1'+m_1'\right)\gamma_5\left(-\not{p}_2+m_2\right)\right]. \end{aligned} \tag{50}$$

By comparing Eq. (42) and Eqs. (49), (50), we have $S_{V(A)}^{B_c\,{}^iA} = S_{A(V)}^{B_cV}(i=1,3)$ with the replacements $m_1''\to -m_1''$, $W_V''\to W''_{{}^3A,{}^1A}$. Note that only the term $1/W''$ is kept in $S_{\mu\nu}^{B_c\,{}^1A}$. Thus the $B_c\to {}^iA(i=1,3)$ form factors can be related to the $B_c\to V$ form factors through the following replacements:

$$\begin{aligned} l^{{}^3A,{}^1A}(q^2) = f(q^2), \quad \text{with} \\ m_1''\to -m_1'', h_V''\to h''_{{}^3A,{}^1A}, w_V''\to w''_{{}^3A,{}^1A}, \end{aligned} \tag{51}$$

$$q^{^3A,^1A}(q^2) = g(q^2), \quad \text{with} \quad m_1'' \to -m_1'', h_V'' \to h''_{^3A,^1A}, w_V'' \to w''_{^3A,^1A}, \tag{52}$$

$$c_\pm^{^3A,^1A}(q^2) = a_\pm(q^2), \quad \text{with} \quad m_1'' \to -m_1'', h_V'' \to h''_{^3A,^1A}, w_V'' \to w''_{^3A,^1A}, \tag{53}$$

where the replacement of $m_1'' \to -m_1''$ is not applied to m_1'' in w'' and h'', because they arise from the propagator and quark–antiquark–meson coupling vertex. The physical form factors $A^{B_cA}(q^2)$, $V_0^{B_cA}(q^2)$, $V_1^{B_cA}(q^2)$, $V_2^{B_cA}(q^2)$ can be related to the above formulae through Eqs. (22) and (23).

We finally turn to the $B_c \to S$ transition amplitude, which is given as [11]

$$\mathcal{B}^{B_cS} = -i^3 \frac{N_c}{(2\pi)^4} \int d^4p_1' \frac{H'_{B_c}\left(H''_S\right)}{N_1' N_1'' N_2} S_\mu^{B_cS}, \tag{54}$$

where the trace $S_\mu^{B_cS}$

$$\begin{aligned} S_\mu^{B_cS} &= Tr\left[\left(\not{p}_1'' + m_1''\right)\gamma_\mu\gamma_5\left(\not{p}_1' + m_1'\right)\gamma_5\left(-\not{p}_2 + m_2\right)\right] \\ &= 2p'_{1\mu}\Big[M'^2 + M''^2 - q^2 - 2N_2 - \left(m_1' - m_2\right)^2 \\ &\quad - \left(m_1'' + m_2\right)^2 + \left(m_1' + m_1''\right)^2\Big] \\ &\quad + q_\mu\Big[q^2 - 2M'^2 + N_1' - N_1'' + 2N_2 + 2\left(m_1' - m_2\right)^2 \\ &\quad - \left(m_1' + m_1''\right)^2\Big] \\ &\quad + P_\mu\Big[q^2 - N_1' - N_1'' - \left(m_1' + m_1''\right)^2\Big]. \end{aligned} \tag{55}$$

Using the formulae above and the integration rules obtained in Refs. [10,11], we have the $B_c \to S$ form factors

$$\begin{aligned} F_1^{B_cS}\left(q^2\right) &= \frac{N_c}{16\pi^3}\int \mathrm{d}x_2 d^2p'_\perp \frac{h'_{B_c}h''_S}{x_2\hat{N}_1'\hat{N}_1''}\left[x_1\left(M_0'^2 + M_0''^2\right) + x_2q^2\right. \\ &\quad \left. - x_2\left(m_1' + m_1''\right)^2 - x_1\left(m_1' - m_2\right)^2 - x_1\left(m_1'' + m_2\right)^2\right], \end{aligned} \tag{56}$$

$$\begin{aligned} F_0^{B_cS}\left(q^2\right) &= F_1^{B_cS}\left(q^2\right) + \frac{q^2}{q\cdot P}\frac{N_c}{16\pi^3}\int \mathrm{d}x_2 d^2p'_\perp \frac{2h'_{B_c}h''_S}{x_2\hat{N}_1'\hat{N}_1''} \\ &\quad \times\Big\{-x_1x_2M'^2 - p_\perp'^2 - m_1'm_2 \\ &\quad - \left(m_1'' + m_2\right)\left(x_2m_1' + x_1m_2\right) \\ &\quad + 2\frac{q\cdot P}{q^2}\left(p_\perp'^2 + 2\frac{\left(p'_\perp\cdot q_\perp\right)^2}{q^2}\right) + 2\frac{\left(p'_\perp\cdot q_\perp\right)^2}{q^2} \\ &\quad - \frac{p'_\perp\cdot q_\perp}{q^2}\left[M''^2 - x_2\left(q^2 + q\cdot P\right)\right. \\ &\quad - \left(x_2 - x_1\right)M'^2 + 2x_1M_0'^2 \\ &\quad \left. -2\left(m_1' - m_2\right)\left(m_1' - m_1''\right)\right]\Big\}. \end{aligned} \tag{57}$$

3 Numerical results and discussions

Equipped with explicit expressions of the form factors $f_+(q^2)$, $f_-(q^2)$ for $B_c \to P$ transitions, $g(q^2)$, $f(q^2)$, $a_+(q^2)$, $a_-(q^2)$ for $B_c \to V$ transitions, $l^{\,^iA}(q^2)$, $q^{\,^iA}(q^2)$, $c_+^{\,^iA}(q^2)$, $c_-^{\,^iA}(q^2)$ for $B_c \to {}^iA(i = 1, 3)$ transitions, and $F_1^{B_cS}(q^2)$, $F_0^{B_cS}(q^2)$ for $B_c \to S$ transitions, we now proceed to perform numerical studies using the CLFQM. In the earlier works [12,13], the form factors of B_c decays into the ground-state charmonia and charmed mesons were calculated. In this work, besides updating the transition form factors of B_c decays to these ground-state charmonia and charmed mesons, we also study the results of B_c transitions to some excited-state charmonia. With these form factors, we then calculate the branching ratios of 80 B_c decays with a charmonium involved in each channel.

As mentioned earlier, the shape parameter β' in the wave function describes the momentum distribution and can be calculated using the meson's decay constant under the CLFQM. The analytic expressions for the calculations are listed in Sect. 2.2. The decay constant for the B_c meson is employed by the result provided by the lattice QCD [38]

$$f_{B_c} = (489 \pm 4 \pm 3)\ \text{MeV}, \tag{58}$$

which is larger than the value used in Refs. [12,13]. The decay constant of J/Ψ can be determined by the leptonic decay width

$$\Gamma_{ee} \equiv \Gamma(J\Psi \to e^+e^-) = \frac{4\pi\alpha_{em}^2 Q_c^2 f_{J\Psi}^3}{3m_{J\Psi}}, \tag{59}$$

with the electric charge of the charm quark $Q_c = \frac{2}{3}$, α_{em} being a fine-structure constant. Using the updated measured result for the electronic width of J/Ψ given in PDG22 [39] $\Gamma_{ee} = (5.53 \pm 0.10)$ keV, one can obtain the decay constant of J/Ψ

$$f_{J/\Psi} = (431.0 \pm 4.3)\ \text{MeV}, \tag{60}$$

which is different from the previous value $f_{J/\Psi} = (416 \pm 5)$ MeV [12]. Similarly, using the measured result $\Gamma(\psi(2S) \to e^+e^-) = 2.36 \pm 0.04$ keV, we obtain the decay constant of the radially excited meson $\psi(2S)$, $f_{\psi(2S)} = 296^{+3}_{-2}$ MeV. The decay constant of the radially excited state $\psi(3S)$ is determined as $f_{\psi(3S)} = (187 \pm 8)$ MeV by using the data $\Gamma_{\psi(3S)\to ee} = (5.53 \pm 0.10)$ keV. As for the decay constant f_{η_c}, we use the lattice QCD results given in Ref. [40]

$$f_{\eta_c} = (387 \pm 7 \pm 2)\ \text{MeV}, \tag{61}$$

which is a little larger than the value $f_{\eta_c} = 340.9^{+16.3}_{-16.6}$ MeV extracted from the data of $\eta_c \to \gamma\gamma$ decay. The decay constant $f_{\eta_c(2S)}$ can be determined by the double photon decay of $\eta_c(2S)$ as

Table 2 The masses (GeV) of the constituent quarks and mesons [39, 41]

m_u	m_d	m_s	m_c	m_b
0.25	0.25	0.37	1.4	4.8
m_{B_c}	m_{D^+}	$m_{D_s^+}$	$m_{D^{*+}}$	$m_{D_s^{*+}}$
6.27447	1.86966	1.96835	2.01026	2.1122
$m_{J/\Psi}$	$m_{\psi(2S)}$	$m_{\psi(3S)}$	$m_{\chi_{c0}}$	$m_{\chi_{c1}}$
3.09690	3.68610	4.039	3.41471	3.51067
m_{η_c}	$m_{\eta_c(2S)}$	$m_{\eta_c(3S)}$	m_{h_c}	$m_{X(3872)}$
2.9839	3.6375	3.940	3.52538	3.87165

$$f_{\eta_c(2S)} = \sqrt{\frac{81 m_{\eta_c(2S)} \Gamma_{\eta_c(2S)\to\gamma\gamma}}{64\pi\alpha_{em}^2}}. \tag{62}$$

By using the measured results of the branching ratio $Br(\eta_c(2S) \to \gamma\gamma) = (1.9 \pm 1.3) \times 10^{-4}$ and $\Gamma_{\eta_c(2S)} = 11.3^{+3.2}_{-2.9}$ MeV [39], we can obtain the decay constant

$$f_{\eta_c(2S)} = (243^{+79}_{-111})\ \text{MeV}. \tag{63}$$

However, there is no calculation for the decay constant of $\eta_c(3S)$ or the data on $\eta_c(3S) \to \gamma\gamma$ decay used to extract it from experiment. We can fix the decay constant $f_{\eta_c(3S)}$ through the assumption $\frac{f_{\eta_c(3S)}}{f_{\eta_c}} = \frac{f_{\psi(3S)}}{f_{J/\Psi}}$ [41,42] and obtain it as

$$f_{\eta_c(3S)} = (170.0 \pm 8.0)\ \text{MeV}. \tag{64}$$

To determine the shape parameter of χ_{c1}, we use the decay constant $f_{\chi_{c1}} = 185$ MeV evaluated from the light-cone QCD sum rules at the scale $\mu = m_c$ [43]. This value is much smaller than $f_{\chi_{c1}} = 340^{+119}_{-101}$ MeV given in Ref. [13]. So the corresponding shape parameter $\beta'_{\chi_{c1}} = (0.536 \pm 0.023)$ GeV is smaller than the value $\beta'_{\chi_{c1}} = (0.7 \pm 0.1)$ GeV obtained in Ref. [13]. For the charmonia χ_{c0} and h_c, we will assume the same values and introduce an uncertainty of 10% to the shape parameters to compensate the different Lorentz structures, that is $\beta'_{\chi_{c0}} = \beta'_{h_c} = (0.536 \pm 0.023)$ GeV. The decay constant of $X(3872)$ is determined using the branching fractions $Br(B^- \to J\Psi K^-) = (1.026 \pm 0.031) \times 10^{-3}$ and $Br(B^- \to X(3872)K^-) = (2.3 \pm 0.9) \times 10^{-4}$ and is obtained as

$$f_{X(3872)} = (234 \pm 52)\ \text{MeV}, \tag{65}$$

which is lower than $f_{X(3872)} = 329^{+111}_{-95}$ MeV used in the previous CLFQM calculations [14]. The experimental results for the decay constants of charmed mesons are given as [39]

$$f_D = (204.6 \pm 5.0)\ \text{MeV}, \quad f_{D_s} = (257.5 \pm 4.6)\ \text{MeV}. \tag{66}$$

As for the decay constants of the vector charmed meson D^* and D_s^*, we used the lattice QCD results $f_{D^*} = (245 \pm 20^{+3}_{-2})$ MeV and $f_{D_s^*} = (272 \pm 16^{+3}_{-20})$ MeV [44].[1] Using these decay constants and the masses of the constituent quarks and mesons given in Table 2, we can obtain the values of the shape parameters β' for our considered mesons which are listed in Table 3.

From Table 4, we can find that the form factors of B_c transitions to charmed mesons (D, D^*, D_s, D_s^*) at the maximally recoiling point ($q^2 = 0$) are smaller than those of B_c transitions to ground-state charmonia. This is because the initial charm quark in the B_c decays to charmed mesons is almost at rest, and its momentum is of order m_c, while the charmed mesons in the final states move very fast, and the final charm quark tends to have a very large momentum of order m_b. So the overlaps of the initial and final states' light-front wave functions in these transitions are limited, which induces small values for the form factors. In the B_c transitions to charmonia, both the spectator charm quark and the charm antiquark generated from the weak vertex are heavy, and the light-front wave functions of the charmonia have a maximum near $E \sim m_c$. It is expected that the overlaps of the B_c and charmonium's light-front wave functions become large, which induces larger form factors. Thus it is easy to understand that for the B_c decays to the charmonium and charmed meson, for example $B_c \to J/\Psi D$, the Feynman amplitudes associated with B_c transitions to charmonia are much more important than that associated with B_c transitions to charmed mesons. Furthermore, the SU(3) symmetry breaking effects between the form factors of $B_c \to D$ and $B_c \to D_s$ transitions are large, since the decay constant of the D_s meson is larger than that of the D meson. It is similar between the form factors of $B_c \to D^*$ and $B_c \to D_s^*$ transitions. These can be checked by future experiments. The uncertainties from the decay constant of $\eta_c(2S)$ shown in Eq. (63) are very large, so there are relevant large uncertainties in the $B_c \to \eta_c(2S)$ transition form factors. It is noted that if evaluating the form factors at the $q^2 > 0$ region in the frame of $q_\perp = 0$, we must include the non-valence configuration (the so-called Z-graph contribution) arising from quark pair creation from the vacuum, which is difficult for us to calculate reliably, while if one calculates in the frame of $q^+ = 0$, such non-valence contribution vanishes automatically. Because of the condition $q^+ = 0$ imposed in the course of calculation, the form factors are obtained only for space-like momentum transfer $q^2 = -q_\perp^2 \le 0$, while the physical transition processes are relevant for the time-like form factors. Many authors [10–12] have proposed parameterization of form factors by using some explicit functions of q^2 in the space-like region, then extending them to the time-like region. Here, we will adopt the parameterization form given in Ref. [12]:

[1] It is noted that all the charmed mesons appearing in this paper are positively charged. In some places, we will omit the sign of charge for simplicity.

Table 3 The shape parameters β' (in units of GeV) in the Gaussian-type light-front wave functions defined in Eq. (25), and the uncertainties are from the decay constants

β'_{B_c}	β'_{D}	β'_{D_s}	β'_{D^*}	$\beta'_{D_s^*}$
$1.058^{+0.009}_{-0.010}$	$0.464^{+0.011}_{-0.014}$	$0.497^{+0.032}_{-0.028}$	$0.409^{+0.021}_{-0.022}$	$0.438^{+0.016}_{-0.027}$
$\beta'_{J/\Psi}$	$\beta'_{\psi(2S)}$	$\beta'_{\psi(3S)}$	β'_{η_c}	$\beta'_{\eta_c(2S)}$
$0.646^{+0.041}_{-0.041}$	$0.566^{+0.004}_{-0.003}$	$0.449^{+0.012}_{-0.013}$	0.754 ± 0.014	$0.488^{+0.140}_{-0.187}$
$\beta'_{\eta_c(3s)}$	$\beta'_{\chi c0}$	$\beta'_{\chi c1}$	β'_{h_c}	$\beta'_{X(3872)}$
$0.382^{+0.045}_{-0.054}$	0.536 ± 0.023	0.536 ± 0.023	0.536 ± 0.023	$0.62^{+0.057}_{-0.064}$

Table 4 $B_c \to D, D^*, D_s, D_s^*, \eta_c, \eta_c(2\,S, 3\,S), J/\Psi, \psi(2\,S, 3\,S)$ form factors in the CLFQM. The uncertainties are from the decay constants of B_c and final-state meson

F	F(0)	$F(q^2_{\max})$	a	b
$F_1^{B_c\eta_c}$	$0.60^{+0.00+0.01}_{-0.00-0.01}$	$1.06^{+0.00+0.03}_{-0.00-0.03}$	$1.95^{+0.01+0.03}_{-0.01-0.03}$	$0.48^{+0.00+0.01}_{-0.00-0.01}$
$F_0^{B_c\eta_c}$	$0.60^{+0.00+0.01}_{-0.01-0.00}$	$0.85^{+0.00+0.02}_{-0.01-0.02}$	$1.44^{+0.00+0.03}_{-0.00-0.03}$	$-0.62^{+0.02+0.02}_{-0.02-0.03}$
$F_1^{B_c\eta_c(2S)}$	$0.37^{+0.00+0.12}_{-0.00-0.18}$	$0.48^{+0.00+0.28}_{-0.00-0.31}$	$1.44^{+0.00+0.92}_{-0.00-0.66}$	$0.15^{+0.02+0.50}_{-0.02-0.34}$
$F_0^{B_c\eta_c(2S)}$	$0.37^{+0.00+0.12}_{-0.00-0.18}$	$0.41^{+0.00+0.28}_{-0.01-0.28}$	$0.73^{+0.01+0.99}_{-0.01-0.95}$	$-0.81^{+0.02+0.34}_{-0.02-0.28}$
$F_1^{B_c\eta_c(3S)}$	$0.29^{+0.00+0.04}_{-0.00-0.05}$	$0.36^{+0.00+0.07}_{-0.00-0.08}$	$1.53^{+0.00+0.29}_{-0.00-0.23}$	$0.23^{+0.01+0.13}_{-0.01-0.13}$
$F_0^{B_c\eta_c(3S)}$	$0.29^{+0.00+0.04}_{-0.00-0.05}$	$0.32^{+0.00+0.07}_{-0.00-0.08}$	$0.85^{+0.01+0.44}_{-0.01-0.31}$	$-0.74^{+0.01+0.05}_{-0.00-0.24}$
$F_1^{B_cD}$	$0.17^{+0.00+0.01}_{-0.00-0.01}$	$0.97^{+0.01+0.10}_{-0.01-0.08}$	$3.09^{+0.02+0.07}_{-0.02-0.05}$	$0.91^{+0.00+0.02}_{-0.00-0.01}$
$F_0^{B_cD}$	$0.17^{+0.00+0.01}_{-0.00-0.01}$	$0.30^{+0.01+0.04}_{-0.01-0.04}$	$2.32^{+0.01+0.08}_{-0.01-0.06}$	$-2.42^{+0.06+0.11}_{-0.06-0.16}$
$F_1^{B_cD_s}$	$0.21^{+0.00+0.01}_{-0.00-0.01}$	$1.09^{+0.01+0.07}_{-0.01-0.06}$	$2.68^{+0.02+0.04}_{-0.01-0.04}$	$0.79^{+0.00+0.01}_{-0.00-0.01}$
$F_0^{B_cD_s}$	$0.21^{+0.00+0.01}_{-0.00-0.01}$	$0.45^{+0.01+0.03}_{-0.01-0.03}$	$1.91^{+0.04+0.01}_{-0.04-0.01}$	$-1.55^{+0.04+0.06}_{-0.04-0.06}$
$V^{B_cJ/\Psi}$	$0.76^{+0.00+0.04}_{-0.00-0.04}$	$1.37^{+0.00+0.11}_{-0.00-0.10}$	$2.16^{+0.01+0.09}_{-0.01-0.08}$	$0.53^{+0.00+0.01}_{-0.00-0.01}$
$A_0^{B_cJ/\Psi}$	$0.55^{+0.00+0.03}_{-0.00-0.04}$	$0.76^{+0.00+0.06}_{-0.00-0.07}$	$1.22^{+0.02+0.07}_{-0.02-0.07}$	$0.16^{+0.00+0.00}_{-0.00-0.00}$
$A_1^{B_cJ/\Psi}$	$0.53^{+0.00+0.02}_{-0.03-0.00}$	$0.78^{+0.01+0.02}_{-0.01-0.05}$	$1.45^{+0.03+0.09}_{-0.01-0.09}$	$0.29^{+0.00+0.02}_{-0.00-0.00}$
$A_2^{B_cJ/\Psi}$	$0.49^{+0.00+0.00}_{-0.00-0.01}$	$0.84^{+0.00+0.03}_{-0.00-0.00}$	$1.97^{+0.01+0.11}_{-0.01-0.11}$	$0.43^{+0.00+0.03}_{-0.00-0.03}$
$V^{B_c\psi(2S)}$	$0.57^{+0.00+0.01}_{-0.00-0.00}$	$0.67^{+0.00+0.02}_{-0.00-0.00}$	$1.01^{+0.01+0.01}_{-0.01-0.02}$	$-0.16^{+0.03+0.01}_{-0.03-0.02}$
$A_0^{B_c\psi(2S)}$	$0.41^{+0.00+0.00}_{-0.00-0.00}$	$0.44^{+0.00+0.00}_{-0.00-0.00}$	$0.39^{+0.01+0.01}_{-0.01-0.01}$	$-0.15^{+0.02+0.01}_{-0.02-0.01}$
$A_1^{B_c\psi(2S)}$	$0.35^{+0.00+0.00}_{-0.00-0.00}$	$0.35^{+0.00+0.00}_{-0.00-0.00}$	$0.08^{+0.01+0.02}_{-0.02-0.03}$	$-0.69^{+0.03+0.01}_{-0.04-0.02}$
$A_2^{B_c\psi(2S)}$	$0.17^{+0.00+0.00}_{-0.00-0.00}$	$0.12^{+0.00+0.00}_{-0.00-0.00}$	$-1.53^{+0.07+0.09}_{-0.09-0.13}$	$-3.67^{+0.14+0.13}_{-0.19-0.21}$
$V^{B_c\psi(3S)}$	$0.46^{+0.00+0.02}_{-0.00-0.02}$	$0.53^{+0.00+0.03}_{-0.00-0.03}$	$1.14^{+0.03+0.04}_{-0.03-0.03}$	$-0.01^{+0.01+0.01}_{-0.01-0.01}$
$A_0^{B_c\psi(3S)}$	$0.31^{+0.00+0.01}_{-0.00-0.01}$	$0.33^{+0.00+0.01}_{-0.00-0.01}$	$0.49^{+0.03+0.03}_{-0.02-0.03}$	$-0.04^{+0.01+0.01}_{-0.01-0.01}$
$A_1^{B_c\psi(3S)}$	$0.27^{+0.00+0.01}_{-0.00-0.01}$	$0.28^{+0.00+0.02}_{-0.00-0.01}$	$0.25^{+0.02+0.04}_{-0.02-0.03}$	$-0.45^{+0.01+0.00}_{-0.01-0.00}$
$A_2^{B_c\psi(3S)}$	$0.14^{+0.00+0.01}_{-0.00-0.01}$	$0.12^{+0.00+0.02}_{-0.00-0.02}$	$-1.01^{+0.02+0.04}_{-0.02-0.04}$	$-2.73^{+0.01+0.00}_{-0.01-0.00}$
$V^{B_cD^*}$	$0.20^{+0.03+0.00}_{-0.03-0.00}$	$1.18^{+0.19+0.10}_{-0.19-0.07}$	$3.39^{+0.02+0.15}_{-0.02-0.12}$	$0.99^{+0.01+0.04}_{-0.01-0.03}$
$A_0^{B_cD^*}$	$0.14^{+0.00+0.02}_{-0.00-0.02}$	$0.35^{+0.01+0.07}_{-0.01-0.06}$	$1.88^{+0.03+0.12}_{-0.03-0.10}$	$0.18^{+0.01+0.01}_{-0.01-0.01}$
$A_1^{B_cD^*}$	$0.13^{+0.02+0.00}_{-0.02-0.00}$	$0.44^{+0.07+0.04}_{-0.07-0.03}$	$2.38^{+0.02+0.16}_{-0.02-0.13}$	$0.52^{+0.00+0.05}_{-0.00-0.04}$
$A_2^{B_cD^*}$	$0.12^{+0.01+0.00}_{-0.00-0.01}$	$0.55^{+0.05+0.05}_{-0.01-0.09}$	$2.98^{+0.02+0.17}_{-0.02-0.15}$	$0.68^{+0.00+0.06}_{-0.00-0.06}$
$V^{B_cD_s^*}$	$0.25^{+0.00+0.00}_{-0.00-0.00}$	$1.24^{+0.01+0.08}_{-0.01-0.05}$	$3.22^{+0.02+0.16}_{-0.02-0.09}$	$0.94^{+0.01+0.04}_{-0.00-0.02}$
$A_0^{B_cD_s^*}$	$0.18^{+0.02+0.00}_{-0.03-0.00}$	$0.41^{+0.05+0.02}_{-0.07-0.01}$	$1.77^{+0.02+0.13}_{-0.02-0.07}$	$0.19^{+0.01+0.01}_{-0.01-0.00}$
$A_1^{B_cD_s^*}$	$0.16^{+0.00+0.01}_{-0.02-0.00}$	$0.47^{+0.00+0.07}_{-0.06-0.02}$	$2.25^{+0.02+0.17}_{-0.02-0.09}$	$0.50^{+0.00+0.05}_{-0.00-0.03}$
$A_2^{B_cD_s^*}$	$0.15^{+0.01+0.00}_{-0.01-0.00}$	$0.60^{+0.05+0.06}_{-0.03-0.04}$	$2.85^{+0.02+0.19}_{-0.02-0.10}$	$0.67^{+0.00+0.06}_{-0.00-0.04}$

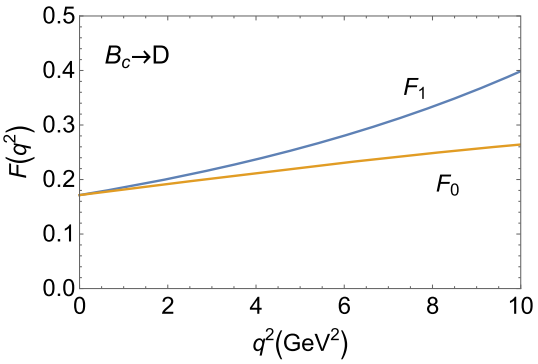

Fig. 2 Form factors $F_1(q^2)$, $F_0(q^2)$ for the $B_c \to D$ transition

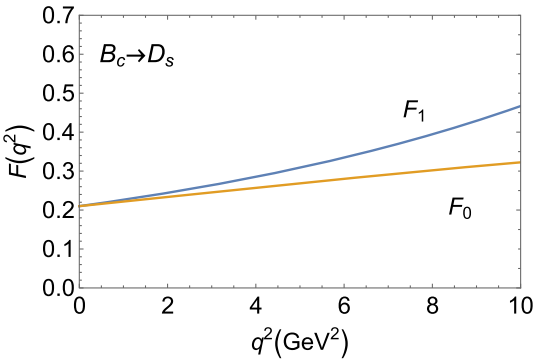

Fig. 3 Form factors $F_1(q^2)$, $F_0(q^2)$ for the $B_c \to D_s$ transition

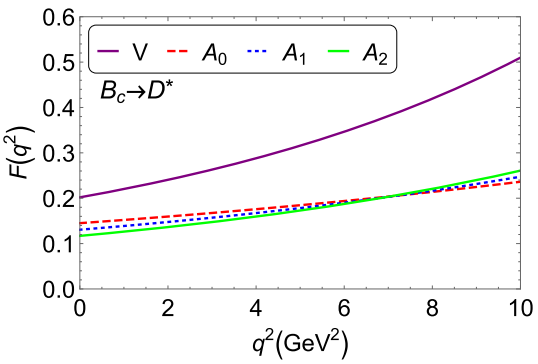

Fig. 4 Form factors $V(q^2)$, $A_0(q^2)$, $A_1(q^2)$ and $A_2(q^2)$ for the $B_c \to D^*$ transition

$$F(q^2) = F(0)\exp\left(a\frac{q^2}{m_{B_c}^2} + b\frac{q^4}{m_{B_c}^4}\right). \tag{67}$$

The parameters a and b will be fitted in the space-like region ($-10\ \text{GeV}^2 \le q^2 \le 0$). The q^2 dependence of form factors in the time-like region are plotted in Figs. 2, 3, 4, 5, 6, 7, 8, 9, 10, and 11. In general the slope parameters a, b are very sensitive to the values of β', while the form factors at $q^2 = 0$ are less sensitive to the variation in β' values.

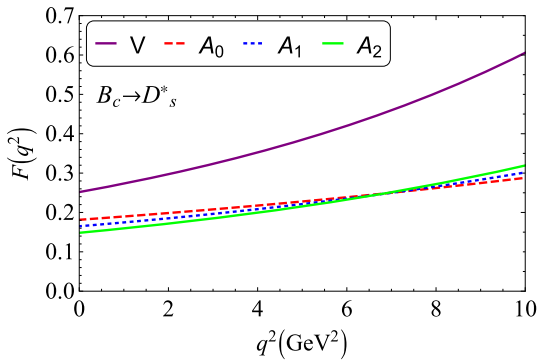

Fig. 5 Form factors $V(q^2)$, $A_0(q^2)$, $A_1(q^2)$ and $A_2(q^2)$ for the $B_c \to D_s^*$ transition

3.1 Transition form factors

In Table 5, we can find that the values of the $B_c \to \eta_c$ transition form factors $F_{0,1}^{B_c\eta_c}$ predicted by many works [12, 45–56] are larger than 0.5, only a few of the values [57–61] are less than 0.5. Similarly, many predictions for the form factor $V^{B_cJ/\psi}$ are larger than 0.6 except for a few values. As for the form factors $A_{0,1,2}^{B_cJ/\psi}$, most of their values lie in the range of $0.5 \sim 0.7$.

In Table 6, we compare our results of the $B_c \to D, D^*, D_s, D_s^*$ transition form factors at $q^2 = 0$ with other calculations. One can find that our results are consistent with those calculated using the relativistic quark model (RQM) [57,58], while they are too large for the results given by the relativistic constituent quark model (RCQM) [52], the light-cone sum rule (LCSR) [53,54], and the QCD sum rules [55,56]. In Refs. [55,56], the form factors have a threefold enhancement by including the Coulomb-like α_s/v corrections for the heavy quarkonium B_c. It seems too small for the values of $F_{0,1}^{B_cD}$ predicted using the Bauer–Stech–Wirbel (BSW) relativistic quark model [48]. Compared with the previous CLFQM calculations [12], our predictions for the form factors $V^{B_cD^*}$, $A_{0,1,2}^{B_cD^*}$ have a significant enhancement by using a larger decay constant f_{D^*}, while the influence from the difference values for the decay constant f_{B_c} is small.

For the B_c transition to a ground-state vector meson, which is either a charmed meson or a charmonium, the form factor V is the largest one, and $A_{0,1,2}$ are close to each other. It is easy to find this character in Figs. 4 and 5 and the first panel of Fig. 7. On the other hand, if the final-state meson is a radially excited meson $\psi(2S)$ or $\psi(3S)$, the form factors show a hierarchy $V > A_2 > A_1 > A_0$, which can be found in the last two panels of Fig. 7. Nevertheless, V is always the largest one among the form factors of the B_c transition to either a ground state or a radially excited charmonium. There also

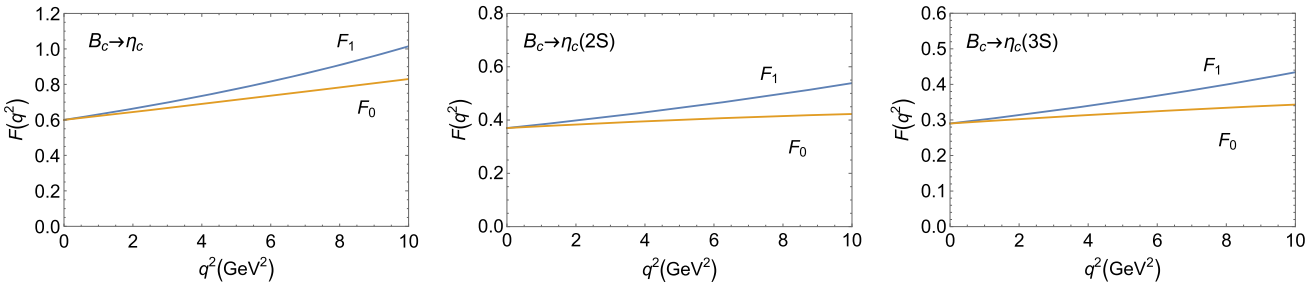

Fig. 6 Form factors $F_1(q^2)$, $F_0(q^2)$ for the $B_c \to \eta_c$ (left), $B_c \to \eta_c(2S)$ (center), and $B_c \to \eta_c(3S)$ (right) transitions

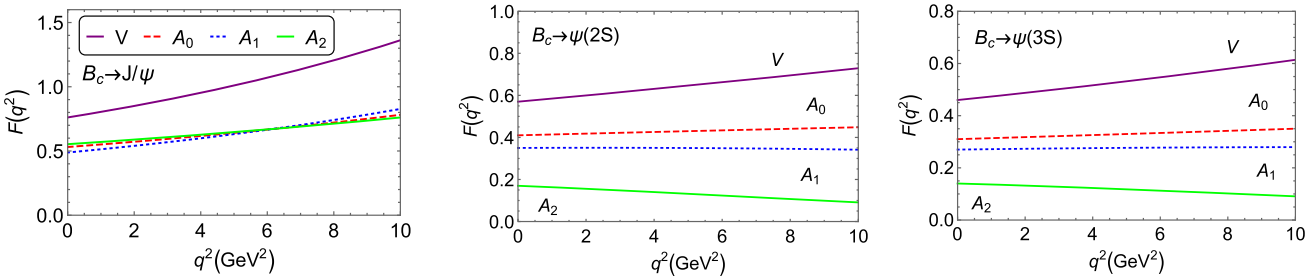

Fig. 7 Form factors $V(q^2)$, $A_0(q^2)$, $A_1(q^2)$ and $A_2(q^2)$ for the $B_c \to J/\Psi$ (left), $B_c \to \psi(2\,S)$ (center) and $B_c \to \psi(3\,S)$ (right) transitions

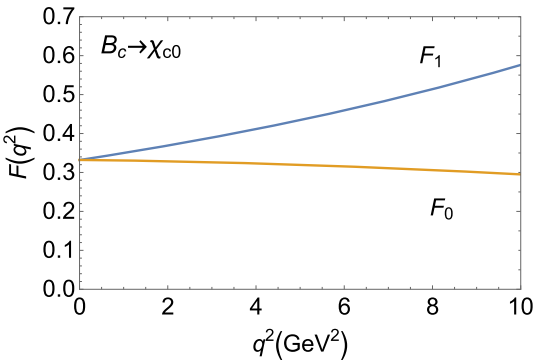

Fig. 8 Form factors$F_1(q^2)$, $F_0(q^2)$ for the $B_c \to \chi_{c0}$ transition

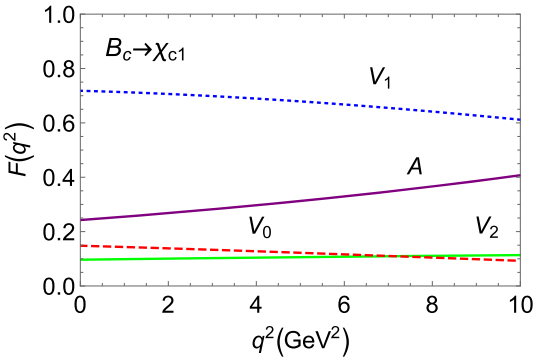

Fig. 9 Form factors $A(q^2)$, $V_0(q^2)$, $V_1(q^2)$, and $V_2(q^2)$ for the $B_c \to \chi_{c1}$ transition

exists another hierarchy for the $B_c \to \eta_c, \eta_c(2S), \eta_c(3S)$ transitions, $F_{0,1}^{B_c\to\eta_c} > F_{0,1}^{B_c\to\eta_c(2\,S)} > F_{0,1}^{B_c\to\eta_c(3\,S)}$. The q^2 dependence of the $B_c \to \chi_{c1}$ transition is shown in Fig. 9, where V_1 is much larger than other form factors A, $V_{0,2}$.

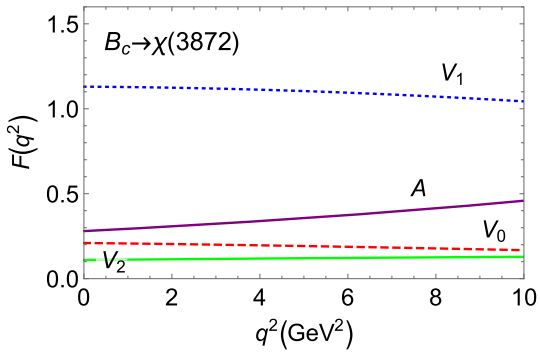

Fig. 10 Form factors $A(q^2)$, $V_0(q^2)$, $V_1(q^2)$ and $V_2(q^2)$ for the $B_c \to X(3872)$ transition

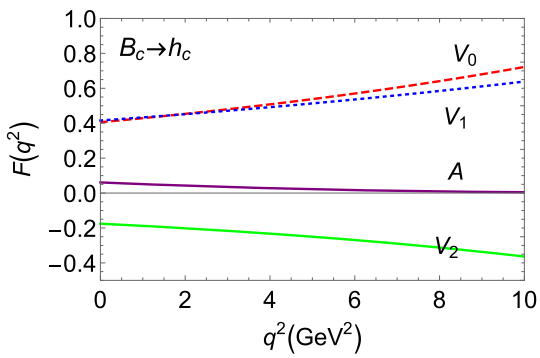

Fig. 11 Form factors $A(q^2)$, $V_0(q^2)$, $V_1(q^2)$, and $V_2(q^2)$ for the $B_c \to h_c$ transition

It is very like the case of the $B_c \to X(3872)$ transition shown in Fig. 10. Thus it is a natural assignment of this state as the first radial excitation of a 1P charmonium state χ_{c1}.

Because both χ_{c1} and $X(3872)$ have the same quantum numbers $J^{PC} = 1^{++}$, they should have similar properties in B_c decays, while it is very different for the B_c transition to another type of axial vector meson h_c with $J^{PC} = 1^{+-}$, where the value of V_0 is large and close to that of V_1 as shown in Fig. 11. Certainly, the values of the form factor V_1 for both B_c transitions to these two types of axial vector charmonia are large. By comparing with Figs. 10 and 11, one can find that both of the values of V_2 in the $B_c \to X(3873)$ and $B_c \to h_c$ transition form factors are the smallest; specifically, V_2 for the $B_c \to h_c$ transition becomes negative. As we know, there is sill no definite answer about the internal properties of the $X(3872)$. From Fig. 10, one can find that the form factors of the $B_c \to X(3872)$ transition are almost flat in their q^2 behaviors except for $A^{B_c X(3872)}$. A comparison of these values with experimental measurements for the $B_c \to X(3872)$ transition form factors will provide unique insight into the mysterious inner structure of $X(3872)$. The form factors for the B_c to these P-wave charmonium transitions are listed in Table 7.

From Table 8, we can find that the form factors of $B_c \to \eta_c(2S, 3S)$, $\psi(2S, 3S)$ transitions calculated in the PQCD approach [29] may be more than twice as large as those predicted in the CLFQM, which will induce large differences for the branching ratios of some correlative decay channels given by these two approaches. In the PQCD approach, the form factors are sensitive to the formulae of the B_c wave functions. In Ref. [29], the authors argued that the B_c wave function in the light-cone formula is broader in shape than that of the traditional zero-point one, which is $\propto \delta(x - r_c)$, so the overlap between the initial and final states' wave functions becomes larger by using the light-cone wave function for the B_c meson, which induces larger form factors. Our predictions for the B_c to vector charmonium J/Ψ, $\psi(2S)$ transition form factors are closer to the results given by the LFQM calculations [15] except for $A_2^{B_c\psi(2S)}$. For the B_c to the axial vector charmonium transition form factors, our results are also consistent with the previous CLQM calculations [13,14].

3.2 Branching ratios

Besides the masses of the constituent quarks and mesons listed in Table 2, other inputs, such as the B_c meson lifetime τ_{B_c}, the Wilson coefficients a_1, a_2, and the Cabibbo–Kobayashi–Maskawa (CKM) matrix elements, are listed as [39,62]

$$\tau_{B_c} = (0.510 \pm 0.009) \times 10^{-12} s, a_1 = 1.07, a_2 = 0.234, \tag{68}$$

$$V_{cd} = 0.221 \pm 0.004, V_{cb} = (40.8 \pm 1.4) \times 10^{-3}, \\ V_{cs} = 0.975 \pm 0.006 \tag{69}$$

$$V_{us} = 0.2243 \pm 0.0008, V_{ud} = 0.97373 \pm 0.00031. \tag{70}$$

First, we consider the branching ratios of the decays $B_c \to \eta_c(J/\Psi)P(V)$, which can be calculated through the formula

$$\mathcal{B}r(B_c \to \eta_c(J/\Psi)P(V)) = \frac{\tau_{B_c}}{\hbar}\Gamma(B_c \to \eta_c(J/\Psi)P(V)), \tag{71}$$

where the decay width $\Gamma(B_c \to \eta_c(J/\Psi)P(V))$ for each channel is given as follows

$$\Gamma(B_c \to \eta_c P(V)) = \frac{\left|G_F V_{cb} V_{uq}^* a_1 f_{P(V)} m_{B_c}^2 F_0^{B_c\eta_c}(m_{P(V)}^2)\right|^2}{32\pi m_{B_c}} \left(1 - r_{\eta_c}^2\right), \tag{72}$$

$$\Gamma(B_c \to J/\Psi P) = \frac{\left|G_F V_{cb} V_{uq}^* a_1 f_P m_{B_c}^2 A_0^{B_c J/\Psi}(m_P^2)\right|^2}{32\pi m_{B_c}} \left(1 - r_{J/\psi}^2\right), \tag{73}$$

with the subscript $q = d(s)$ in the CKM element V_{uq} for the decays with $\pi, \rho(K, K^*)$ involved. For the decays $B_c \to J/\Psi V$, the corresponding decay width is the summation of the three polarizations

$$\Gamma(B_c \to J/\Psi V) = \frac{|\vec{p}|}{8\pi m_{B_c}^2} \left(|\mathcal{A}_L(B_c \to J/\Psi V)|^2 + 2|\mathcal{A}_N(B_c \to J/\Psi V)|^2 + 2|\mathcal{A}_T(B_c \to J/\psi V)|^2\right), \tag{74}$$

where $\vec{p}$ is the three-momentum of either of the two final states in the B_c rest frame

$$|\mathbf{p}| = \frac{\sqrt{\left(m_{B_c}^2 - \left(m_{J/\psi} + m_V\right)^2\right)\left(m_{B_c}^2 - \left(m_{J/\psi} - m_V\right)^2\right)}}{2m_{B_c}}, \tag{75}$$

and the three polarization amplitudes $\mathcal{A}_L, \mathcal{A}_N, and \mathcal{A}_T$ are given as

$$\mathcal{A}_L(B_c \to J/\Psi V) = \frac{G_F}{\sqrt{2}} V_{cb}^* V_{uq} a_1 f_V m_{B_c}^2 \frac{1}{2r_{J/\Psi}} \left[\frac{\lambda(1, r_{J/\Psi}^2, r_V^2)}{1 + r_{J/\Psi}} A_2^{B_c J/\Psi}(m_V^2) - (1 - r_{J/\Psi}^2 - r_V^2)(1 + r_{J/\Psi}) A_1^{B_c J/\Psi}(m_V^2)\right], \tag{76}$$

$$\mathcal{A}_N(B_c^+ \to J/\psi V) = -\frac{G_F}{\sqrt{2}} V_{cb}^* V_{uq} a_1 f_V m_{B_c}^2 r_V \left(1 + r_{J/\Psi}\right) A_1^{B_c J/\Psi}\left(m_V^2\right), \tag{77}$$

Table 5 Comparison of the $B_c \to \eta_c$ and $B_c \to J/\Psi$ transition form factors at $q^2 = 0$ between this work and other literature

	$F_1^{B_c\eta_c} = F_0^{B_c\eta_c}$	$V^{B_cJ/\psi}$	$A_0^{B_cJ/\psi}$	$A_1^{B_cJ/\psi}$	$A_2^{B_cJ/\psi}$
This work	0.60	0.76	0.55	0.53	0.49
[12]	0.61	0.74	0.53	0.50	0.44
[45]	0.5359	0.736	0.532	0.524	0.509
[46]	0.61	0.83	0.57	0.56	0.54
[47][1]	0.66	–	0.655	0.578	0.427
[48]	0.58	0.91	0.58	0.63	0.74
[51]	0.66	1.03	0.60	0.63	0.69
[52]	0.76	0.96	0.69	0.68	0.66
[53,54]	0.87	1.69	0.27	0.75	1.69
[55,56][2]	0.66[0.7]	1.03[0.94]	0.60[0.66]	0.63[0.66]	0.69[0.66]
[57]	0.420	0.591	0.408	0.416	0.431
[58]	0.47	0.49	0.40	0.50	0.73
[59]	0.49	0.61	0.45	0.49	0.56
[60]	0.20	0.38	0.26	0.27	0.28
[61]	0.23	0.33	0.21	0.21	0.23

[1] Here, the results with $\omega = 0.8$ GeV are quoted
[2] The results out (in) the brackets are evaluated in the sum rules (potential) model

Table 6 Comparison of the $B_c \to D, D^*, D_s, D_s^*$ transition form factors at $q^2 = 0$ between this work and other literature

	$F_1^{B_cD} = F_0^{B_cD}$	$A_0^{B_cD^*}$	$A_1^{B_cD^*}$	$A_2^{B_cD^*}$	$V^{B_cD^*}$
This work	0.17	0.20	0.14	0.13	0.12
[60]	0.13	0.25	0.05	0.11	0.17
[58]	0.14	0.18	0.14	0.17	0.19
[45]	0.1446	0.175	0.094	0.100	0.105
[57][1]	0.154	0.224	0.156	0.145	0.134
[12]	0.16	0.13	0.09	0.08	0.07
[55,56][2]	0.32[0.29]	1.66[1.74]	0.35[0.37]	0.43[0.43]	0.51[0.50]
[53,54]	0.35	0.57	0.05	0.32	0.57
[52]	0.69	0.98	0.47	0.56	0.64
[48]	0.075	0.16	0.081	0.095	0.11
	$F_1^{B_cD_s} = F_0^{B_cD_s}$	$A^{B_cD_s^*}$	$V_0^{B_cD_s^*}$	$V_1^{B_cD_s^*}$	$V_2^{B_cD_s^*}$
This work	0.21	0.25	0.18	0.16	0.15
[48]	0.15	0.29	0.16	0.18	0.20
[12]	0.28	0.23	0.17	0.14	0.12
[55,56][2]	0.45[0.43]	2.02[2.27]	0.47[0.52]	0.56[0.56]	0.65[0.60]

[1] Here, the results with $\omega = 0.6$ GeV are quoted
[2] The results out (in) the brackets are evaluated in the sum rules (potential) model

$$\mathcal{A}_T\left(B_c \to J/\Psi V\right) = -\frac{G_F}{\sqrt{2}} V_{cb}^* V_{uq} a_1 f_V m_{B_c}^2 r_V \frac{\sqrt{\lambda\left(1, r_{J/\Psi}^2, r_V^2\right)}}{1 + r_{J/\Psi}} V^{B_cJ/\Psi}\left(m_V^2\right), \tag{78}$$

with $\lambda\left(1, r_{J/\Psi}^2, r_V^2\right) = \left(1 + r_{J/\psi}^2 - r_V^2\right)^2 - 4r_{J/\Psi}^2$.

From Table 9, one can find that our predictions are consistent with the results given by the QCD sum rules [32], the relativistic constituent quark model (RCQM) [34], and the Bethe–Salpeter equation approach under the so-called instantaneous nonrelativistic approximation [33]. In Ref. [36], the authors calculated these decays in the nonrelativistic QCD (NRQCD) approach at the next-to-leading-order (NLO) in the QCD coupling α_s. It is interesting that the leading-order (LO) results for these channels, except for the decay $B_c^+ \to J/\Psi\rho^+$, are in agreement with our predictions, while the branching ratios obtain substantial enhancement

Table 7 Results for the $B_c \to \chi_{c0}, \chi_{c1}, h_c, X(3872)$ transition form factors and the fitted parameters a and b. The uncertainties are from the decay constants of B_c and final-state mesons

F	F(0)	$F(q^2_{\max})$	a	b
$F_1^{B_c\chi_{c0}}$	$0.33^{+0.00+0.02}_{-0.02-0.00}$	$0.52^{+0.00+0.04}_{-0.00-0.03}$	$2.07^{+0.02+0.04}_{-0.02-0.04}$	$0.39^{+0.01+0.01}_{-0.01-0.02}$
$F_0^{B_c\chi_{c0}}$	$0.33^{+0.02+0.02}_{-0.00-0.02}$	$0.30^{+0.02+0.02}_{-0.00-0.02}$	$-0.14^{+0.01+0.06}_{-0.01-0.06}$	$-1.29^{+0.01+0.03}_{-0.01-0.03}$
$A^{B_c\chi_{c1}}$	$0.24^{+0.00+0.01}_{-0.00-0.01}$	$0.36^{+0.00+0.02}_{-0.00-0.02}$	$1.96^{+0.02+0.03}_{-0.02-0.03}$	$0.33^{+0.02+0.01}_{-0.01-0.02}$
$V_0^{B_c\chi_{c1}}$	$0.15^{+0.00+0.00}_{-0.00-0.00}$	$0.11^{+0.00+0.01}_{-0.00-0.00}$	$-1.19^{+0.01+0.20}_{-0.20-0.01}$	$-2.60^{+0.05+0.24}_{-0.05-0.25}$
$V_1^{B_c\chi_{c1}}$	$0.72^{+0.00+0.02}_{-0.00-0.02}$	$0.65^{+0.00+0.02}_{-0.00-0.03}$	$-0.25^{+0.02+0.10}_{-0.02-0.09}$	$-1.51^{+0.00+0.06}_{-0.00-0.06}$
$V_2^{B_c\chi_{c1}}$	$0.10^{+0.00+0.00}_{-0.00-0.00}$	$0.11^{+0.00+0.00}_{-0.00-0.00}$	$0.83^{+0.04+0.02}_{-0.03-0.02}$	$-0.77^{+0.05+0.03}_{-0.03-0.05}$
$A^{B_c h_c}$	$0.06^{+0.00+0.00}_{-0.00-0.00}$	$0.01^{+0.00+0.00}_{-0.00-0.00}$	$-6.24^{+0.08+0.60}_{-0.07-0.66}$	$-14.41^{+0.12+1.46}_{-0.11-1.62}$
$V_0^{B_c h_c}$	$0.41^{+0.03+0.00}_{-0.03-0.00}$	$0.63^{+0.05+0.01}_{-0.05-0.01}$	$2.17^{+0.02+0.05}_{-0.02-0.05}$	$0.38^{+0.01+0.01}_{-0.01-0.02}$
$V_1^{B_c h_c}$	$0.42^{+0.02+0.00}_{-0.02-0.00}$	$0.58^{+0.03+0.01}_{-0.03-0.01}$	$1.64^{+0.02+0.05}_{-0.02-0.0.05}$	$0.22^{+0.00+0.01}_{-0.00-0.01}$
$V_2^{B_c h_c}$	$-0.18^{+0.00+0.01}_{-0.00-0.01}$	$-0.31^{+0.01+0.00}_{-0.00-0.01}$	$2.71^{+0.02+0.04}_{-0.02-0.04}$	$0.61^{+0.01+0.01}_{-0.01-0.02}$
$A^{B_c X(3872)}$	$0.28^{+0.00+0.02}_{-0.00-0.03}$	$0.37^{+0.00+0.03}_{-0.00-0.04}$	$1.85^{+0.02+0.09}_{-0.02-0.08}$	$0.38^{+0.01+0.01}_{-0.01-0.03}$
$V_0^{B_c X(3872)}$	$0.21^{+0.00+0.01}_{-0.00-0.01}$	$0.19^{+0.00+0.02}_{-0.00-0.02}$	$-0.52^{+0.01+0.38}_{-0.01-0.32}$	$-1.45^{+0.02+0.36}_{-0.03-0.32}$
$V_1^{B_c X(3872)}$	$1.13^{+0.00+0.01}_{-0.00-0.03}$	$1.10^{+0.00+0.05}_{-0.00-0.06}$	$-0.05^{+0.01+0.24}_{-0.01-0.20}$	$-1.03^{+0.00+0.15}_{-0.00-0.12}$
$V_2^{B_c X(3872)}$	$0.11^{+0.00+0.01}_{-0.01-0.01}$	$0.12^{+0.00+0.01}_{-0.01-0.01}$	$0.77^{+0.03+0.04}_{-0.03-0.04}$	$-0.61^{+0.02+0.08}_{-0.02-0.12}$

Table 8 Comparison of the $B_c \to \eta_c(2S, 3S), \psi(2S, 3S), \chi_{c1}, h_c, X(3872)$ transition form factors at $q^2 = 0$ between this work and other literature

	$F_1^{B_c\eta_c(2S)}(0) = F_0^{B_c\eta_c(2S)}(0)$	$F_1^{B_c\eta_c(3S)}(0) = F_0^{B_c\eta_c(3S)}(0)$	–	–
This work	0.37	0.29	–	–
[29]	1.04	0.78	–	–
	$V^{B_c\psi(2S)}$	$A_0^{B_c\psi(2S)}$	$A_1^{B_c\psi(2S)}$	$A_2^{B_c\psi(2S)}$
This work	0.57	0.41	0.35	0.17
[15]	0.525	0.452	0.335	0.102
[29]	1.71	0.80	0.87	1.22
	$V^{B_c\psi(3S)}$	$A_0^{B_c\psi(3S)}$	$A_1^{B_c\psi(3S)}$	$A_2^{B_c\psi(3S)}$
This work	0.46	0.31	0.27	0.14
[29]	1.07	0.41	0.41	0.66
	$A^{B_c\chi_{c1}}$	$V_0^{B_c\chi_{c1}}$	$V_1^{B_c\chi_{c1}}$	$V_2^{B_c\chi_{c1}}$
This work	0.24	0.15	0.72	0.10
[13]	0.36	0.13	0.85	0.15
	$A^{B_c h_c}$	$V_0^{B_c h_c}$	$V_1^{B_c h_c}$	$V_2^{B_c h_c}$
This work	0.06	0.41	0.42	−0.18
[13]	0.07	0.64	0.50	−0.32
	$A^{B_c X(3872)}$	$V_0^{B_c X(3872)}$	$V_1^{B_c X(3872)}$	$V_2^{B_c X(3872)}$
This work	0.28	0.21	1.13	0.11
[14]	0.36	0.18	1.15	0.13

after including the NLO QCD correction, which provides a large factor K. We wonder whether these results will still be stable with the higher-order corrections, such as the next-to-next-to-leading-order (NNLO) contributions, involved. In Ref. [63], the branching ratios are calculated in the relativistic quark model using v/c expansion for B_c and the charmonium, and the obtained results are smaller than most of the other predictions, including ours; for example, their results are only about one third of our predictions in most cases. Certainly, the results given in the QCD relativistic (potential) models [66,67] are also small. As mentioned earlier, the results calculated using the PQCD approach are sensitive to the types of wave functions for the B_c meson (the traditional zero-point wave function and the light-cone wave function).

For example, if taking the light-cone wave function for the B_c meson, the branching ratio of the decay $B_c^+ \to \eta_c \pi^+$ will reach $(5.2^{+2.6}_{-1.4}) \times 10^{-3}$ [29], which is much larger than $(2.98^{+1.24}_{-1.05}) \times 10^{-3}$ obtained using the traditional zero-point one. From Table 9, one can find that the ratio of the branching fractions $R_{K/\pi} \equiv \frac{Br(B_c^+ \to J/\Psi K^+)}{Br(B_c^+ \to J/\Psi \pi^+)} = 0.081 \pm 0.011$, which is consistent with the value $R_{K/\pi} = 0.079 \pm 0.007 \pm 0.003$ given by the LHCb collaboration [69].

If replacing $P(V)$ with $D(D^*)$, the branching ratios of the corresponding decays $B_c \to \eta_c(J/\Psi)D(D^*)$ can be obtained by their decay widths:

$$\begin{aligned}
&\Gamma(B_c \to \eta_c D) \\
&= \frac{\left(G_F V_{cb}^* V_{cd} m_{B_c}^2\right)^2 \left(1 - r_{\eta_c}^2 - r_D^2\right)}{32\pi m_{B_c}} \\
&\quad \times |a_1 f_D F_0^{B_c \eta_c}(m_D^2) + a_2 f_{\eta_c} F_0^{B_c D}(m_{\eta_c}^2)|^2, \qquad (79) \\
&\Gamma\left(B_c \to \eta_c D^*\right) \\
&= \frac{\left(G_F V_{cb}^* V_{cd} m_{B_c}^2\right)^2 \left(1 - r_{\eta_c}^2 - r_{D^*}^2\right)}{32\pi m_{B_c}} \\
&\quad \times |a_1 f_{D^*} F_0^{B_c \eta_c}(m_{D^*}^2) + a_2 f_{\eta_c} A_0^{B_c D^*}(m_{\eta_c}^2)|^2, \qquad (80) \\
&\Gamma(B_c \to J/\Psi D) \\
&= \frac{\left(G_F V_{cb}^* V_{cd} m_{B_c}^2\right)^2 \left(1 - r_{J/\psi}^2 - r_D^2\right)}{32\pi m_{B_c}} \\
&\quad \times |a_1 f_D A_0^{B_c J/\Psi}(m_D^2) + a_2 f_{J/\Psi} F_0^{B_c D}(m_{J/\Psi}^2)|^2. \qquad (81)
\end{aligned}$$

For the decay $B_c \to J/\Psi D^*$, the corresponding decay width is the summation of the three polarizations:

$$\begin{aligned}
&\Gamma\left(B_c \to J/\Psi D^*\right) \\
&= \frac{|\mathbf{p}|}{8\pi m_{B_c}^2} \left(|\mathcal{A}_L(B_c \to J/\Psi D^*)|^2 + 2\left|\mathcal{A}_N\left(B_c \to J/\Psi D^*\right)\right|^2\right. \\
&\quad \left. + 2\left|\mathcal{A}_T\left(B_c \to J/\Psi D^*\right)\right|^2\right), \qquad (82)
\end{aligned}$$

where the three polarization amplitudes $\mathcal{A}_L, \mathcal{A}_N, and \mathcal{A}_T$ are given as

$$\begin{aligned}
&\mathcal{A}_L\left(B_c \to J/\Psi D^*\right) \\
&= \frac{G_F}{\sqrt{2}} V_{cb}^* V_{cd} m_{B_c}^2 \left\{ -(1 - r_{J/\Psi}^2 - r_{D^*}^2) \right. \\
&\quad \times \left[\frac{a_1 f_{D^*}(1 + r_{J/\Psi})}{2 r_{J/\Psi}} A_1^{B_c J/\Psi}(m_{D^*}^2) \right. \\
&\quad \left. + \frac{a_2 f_{J/\Psi}(1 + r_{D^*})}{2 r_{D^*}} A_1^{B_c D^*}(m_{J/\Psi}^2) \right] \\
&\quad + \frac{a_1 \lambda_1 f_{D^*}}{2 r_{J/\Psi}(1 + r_{J/\Psi})} A_2^{B_c J/\Psi}(m_{D^*}^2) \\
&\quad \left. + \frac{a_2 \lambda_2 f_{J/\Psi}}{2 r_{D^*}(1 + r_{D^*})} A_2^{B_c D^*}(m_{J/\Psi}^2) \right\}, \qquad (83) \\
&\mathcal{A}_N\left(B_c \to J/\psi D^*\right) \\
&= -\frac{G_F}{\sqrt{2}} V_{cb}^* V_{cd} m_{B_c}^2 \left[a_1 f_{D^*} r_{D^*} \left(1 + r_{J/\Psi}\right) A_1^{B_c J/\Psi}\left(m_{D^*}^2\right) \right. \\
&\quad \left. + a_2 f_{J/\Psi} r_{J/\Psi} \left(1 + r_{D^*}\right) A_1^{B_c D^*}\left(m_{J/\Psi}^2\right) \right], \qquad (84) \\
&\mathcal{A}_T\left(B_c \to J/\Psi D^*\right) \\
&= -\frac{G_F}{\sqrt{2}} V_{cb}^* V_{cd} m_{B_c}^2 \left[\frac{a_1 \sqrt{\lambda_1}}{1 + r_{J/\Psi}} f_{D^*} r_{D^*} V^{B_c J/\Psi}\left(m_{D^*}^2\right) \right. \\
&\quad \left. + \frac{a_2 \sqrt{\lambda_2}}{1 + r_{D^*}} f_{J/\Psi} r_{J/\Psi} V^{B_c D^*}\left(m_{J/\psi}^2\right) \right], \qquad (85)
\end{aligned}$$

with $\lambda_1 = \lambda\left(1, r_{J/\Psi}^2, r_{D^*}^2\right), \lambda_2 = \lambda\left(1, r_{D^*}^2, r_{J/\Psi}^2\right)$. As for the decay widths of the decays $B_c \to \eta_c(J/\Psi)D_s(D_s^*)$, they can be obtained by performing the replacements $D \to D_s, D^* \to D_s^*, V_{cd} \to V_{cs}$ in Eqs. (79)–(85). The calculation results are listed in Table 10. One can find that our predictions are a little larger than most of the other results, but are smaller the the PQCD calculations. The branching ratios of the decays with $D_s^{(*)}$ involved are at least one order larger than those of the corresponding decays with $D^{(*)}$ involved. This is because the CKM matrix element V_{cs} associated with the former is much larger than V_{cd} associated with the latter. All of these decays with the ground-state S-wave charmonia involved have large branching ratios, which lie in the range of $10^{-4} \sim 10^{-3}$ and can be detected by the present LHCb experiments. In Ref. [24], if assuming that the spectator diagram dominates and that factorization holds, one can obtain the approximations

$$R_{D_s^+/\pi^+} \equiv \frac{\Gamma(B_c^+ \to J/\Psi D_s^+)}{\Gamma(B_c^+ \to J/\Psi \pi^+)} \approx \frac{\Gamma(B_c^+ \to \bar{D}^* D_s^+)}{\Gamma(B_c^+ \to \bar{D}^* \pi^+)}, \qquad (86)$$

$$R_{D_s^{*+}/D_s^+} \equiv \frac{\Gamma(B_c^+ \to J/\Psi D_s^{*+})}{\Gamma(B_c^+ \to J/\Psi D_s^+)} \approx \frac{\Gamma(B_c^+ \to \bar{D}^* D_s^{*+})}{\Gamma(B_c^+ \to \bar{D}^* D_s^+)}, \qquad (87)$$

which were measured as $R_{D_s^+/\pi^+} = 2.90 \pm 0.57 \pm 0.24$ and $R_{D_s^{*+}/D_s^+} = 2.37 \pm 0.56 \pm 0.10$ by the LHCb collaboration [24], and given as $R_{D_s^+/\pi^+} = 2.76 \pm 0.47$ and $R_{D_s^{*+}/D_s^+} = 1.93 \pm 0.26$ by ATLAS [71]. From our calculations, these two ratios are obtained as

$$R_{D_s^+/\pi^+} \equiv \frac{\Gamma(B_c^+ \to J/\Psi D_s^+)}{\Gamma(B_c^+ \to J/\Psi \pi^+)} = 3.09 \pm 1.05, \qquad (88)$$

$$R_{D_s^{*+}/D_s^+} \equiv \frac{\Gamma(B_c^+ \to J/\Psi D_s^{*+})}{\Gamma(B_c^+ \to J/\Psi D_s^+)} = 1.48 \pm 0.50, \qquad (89)$$

where the value of $R_{D_s^+/\pi^+}$ is consistent with the measurements given by LHCb and ATLAS, while $R_{D_s^{*+}/D_s^+}$ can explain the ATLAS result within errors.

Next, we consider the decays with the P-wave charmonia involved in the final states. The P-wave charmonium can be χ_{c0}, χ_{c1}, or h_c. The decay widths of the decays $B_c \to \chi_{c0(1)} P(V), h_c P(V)$ are given as follows

Table 9 The CLFQM predictions for branching ratios (10^{-3}) of B_c decays to final states containing a ground-state S-wave charmonium (η_c or J/Ψ) and a light pseudoscalar or vector meson. The first error is induced by the B_c meson life time, and the second and third uncertainties are from the decay constants of B_c and charmonia

Mode	This work	[36]	[63]	[33]	[32]	[34]	[64,65]	[66]	[67]	[68]	[29]	[14]	[15]
$B_c^+ \to J/\psi\pi^+$	$1.97^{+0.04+0.00+0.24}_{-0.04-0.00-0.25}$	2.91(2.22)	0.61	2.1	1.3	1.7	0.34	1.3	1.1	2.33	2.6	2.0	0.664
$B_c^+ \to J/\psi K^+$	$0.16^{+0.00+0.00+0.02}_{-0.00-0.00-0.02}$	0.22(0.16)	0.05	0.16	0.11	0.13	0.11	0.07	0.08	0.19	–	0.16	0.0527
$B_c^+ \to J/\psi\rho^+$	$5.34^{+0.09+0.07+0.73}_{-0.09-0.07-0.63}$	8.08(6.03)	1.6	6.5	4.0	4.9	1.8	3.7	3.1	8.20	–	5.0	–
$B_c^+ \to J/\psi K^{*+}$	$0.31^{+0.01+0.00+0.04}_{-0.01-0.00-0.04}$	0.43(0.32)	0.10	0.35	0.22	0.28	0.09	0.2	0.18	0.48	–	0.29	0.109
$B_c^+ \to \eta_c\pi^+$	$2.36^{+0.04+0.00+0.06}_{-0.04-0.00-0.06}$	5.19(2.95)	0.85	2.2	2.0	1.9	0.34	0.26	1.4	2.98	5.2	–	–
$B_c^+ \to \eta_c K^+$	$0.19^{+0.00+0.00+0.00}_{-0.00-0.00-0.01}$	0.38(0.21)	0.07	0.17	0.13	0.15	0.03	0.02	0.11	0.24	–	–	–
$B_c^+ \to \eta_c\rho^+$	$6.01^{+0.11+0.00+0.16}_{-0.11-0.01-0.16}$	14.5(7.89)	2.1	5.9	4.2	4.5	1.06	0.67	3.3	9.83	–	–	–
$B_c^+ \to \eta_c K^{*+}$	$0.34^{+0.01+0.00+0.01}_{-0.01-0.00-0.01}$	0.77(0.41)	0.11	0.31	0.20	0.25	0.06	0.04	0.18	0.57	–	–	–

Table 10 CLFQM predictions for branching ratios (10^{-3}) of B_c decays to final states containing a ground-state S-wave charmonium (η_c or J/Ψ) and a charmed meson. The errors are induced by the same sources as in Table 9

Mode	This work	[33]	[32]	[34]	[64,65]	[60]	[67]	[70]	[68]
$B_c^+ \to \eta_c D^+$	$0.22^{+0.00+0.01+0.02}_{-0.00-0.01-0.00}$	0.012	0.15	0.19	0.06	0.05	0.14	0.10	0.44
$B_c^+ \to J/\psi D^+$	$0.20^{+0.00+0.00+0.03}_{-0.00-0.00-0.03}$	0.009	0.09	0.15	0.04	0.13	0.09	0.09	0.28
$B_c^+ \to \eta_c D^{*+}$	$0.31^{+0.01+0.00+0.01}_{-0.01-0.00-0.01}$	0.010	0.10	0.19	0.07	0.02	0.13	0.10	0.58
$B_c^+ \to J/\psi D^{*+}$	$0.41^{+0.01+0.00+0.05}_{-0.01-0.00-0.01}$	–	0.28	0.45	0.18	0.19	0.28	0.28	0.67
$B_c^+ \to \eta_c D_s^+$	$6.44^{+0.11+0.73+0.94}_{-0.11-0.71-0.50}$	0.54	2.8	4.4	1.79	5	2.6	2.5	12.32
$B_c^+ \to J/\psi D_s^+$	$6.09^{+0.11+0.36+1.15}_{-0.11-0.33-0.47}$	0.41	1.7	3.4	1.15	3.4	1.5	2.2	8.05
$B_c^+ \to \eta_c D_s^{*+}$	$6.97^{+0.12+0.17+0.39}_{-0.12-0.14-0.07}$	0.44	2.7	3.7	1.49	0.38	2.4	2.0	16.54
$B_c^+ \to J/\psi D_s^{*+}$	$9.03^{+0.04+0.02+0.34}_{-0.04-0.02-0.32}$	–	6.7	9.7	4.4	5.9	5.5	6.0	20.45

$$\Gamma\left(B_c \to \chi_{c0} P(V)\right) = \frac{\left|G_F V_{cb} V_{uq}^* a_1 f_{P(V)} m_{B_c}^2 F_0^{B_c\chi_{c0}}(m_{P(V)}^2)\right|^2}{32\pi m_{B_c}} \left(1 - r_{\chi_{c0}}^2\right), \tag{90}$$

$$\Gamma\left(B_c \to \chi_{c1} P\right) = \frac{\left|G_F V_{cb} V_{uq}^* a_1 f_P m_{B_c}^2 A_0^{B_c\chi_{c1}}(m_P^2)\right|^2}{32\pi m_{B_c}} \left(1 - r_{\chi_{c1}}^2\right), \tag{91}$$

where the subscript $q = d(s)$ in the CKM element V_{uq} for the decays with π, $\rho(K, K^*)$ involved. For the decays $B_c \to \chi_{c1} V$, the corresponding decay widths are the summation of the three polarizations

$$\Gamma\left(B_c \to \chi_{c1} V\right) = \frac{|\vec{p}|}{8\pi m_{B_c}^2}\left(|\mathcal{A}_L(B_c \to \chi_{c1} V)|^2 + 2\,|\mathcal{A}_N\left(B_c \to \chi_{c1} V\right)|^2 + 2\,|\mathcal{A}_T\left(B_c \to \chi_{c1} V\right)|^2\right), \tag{92}$$

where

$$\mathcal{A}_L\left(B_c \to \chi_{c1} V\right) = \frac{G_F}{\sqrt{2}} V_{cb}^* V_{uq} a_1 f_V m_{B_c}^2 \frac{1}{2r_{\chi_{c1}}}\left[\frac{\lambda(1, r_{\chi_{c1}}^2, r_V^2)}{1 - r_{\chi_{c1}}} V_2^{B_c\chi_{c1}}(m_V^2) - (1 - r_{\chi_{c1}}^2 - r_V^2)(1 - r_{\chi_{c1}}) V_1^{B_c\chi_{c1}}(m_V^2)\right], \tag{93}$$

$$\mathcal{A}_N\left(B_c^+ \to \chi_{c1} V\right) = -\frac{G_F}{\sqrt{2}} V_{cb}^* V_{uq} a_1 f_V m_{B_c}^2 r_V \left(1 - r_{\chi_{c1}}\right) V_1^{B_c\chi_{c1}}\left(m_V^2\right), \tag{94}$$

$$\mathcal{A}_T\left(B_c \to \chi_{c1} V\right) = -\frac{G_F}{\sqrt{2}} V_{cb}^* V_{uq} a_1 f_V m_{B_c}^2 r_V \frac{\sqrt{\lambda\left(1, r_{\chi_{c1}}^2, r_V^2\right)}}{1 - r_{\chi_{c1}}} A^{B_c\chi_{c1}}\left(m_V^2\right). \tag{95}$$

It is noted that the analytic formulae of the decay widths between the decays $B_c \to h_c P(V)$ and $B_c \to \chi_{1c} P(V)$ are similar. Summing the branching fractions of the these decays in Table 11, we find that the results of the decays with $\pi^+(\rho^+)$ involved are about one order of magnitude larger compared with those of the decays with $K^+(K^{*+})$ involved. The difference mainly comes from the the CKM matrix elements: the former involve a larger factor $V_{ud} \sim 1$, while the latter is associated with a smaller factor $V_{us} = \lambda \sim 0.225$. Our predictions are comparable to most other theoretical results, such as the QCD-motivated RQM based on the quasi-potential approach [72], the NRQM [59], and the RCQM [73]. The branching ratios of the decays $B_c \to \chi_{c0(1)} P(V)$

Table 11 The CLFQM predictions for branching ratios (10^{-3}) of B_c decays to final states containing a P-wave charmonium and a light pseudoscalar or vector meson. The errors are induced by the same sources as in Table 9

Mode	This work	[72]	[59]	[73]	[74]	[75]	[76]	[28]	[77]
$B_c^+ \to \chi_{c0}\pi^+$	$0.66^{+0.01+0.01+0.08}_{-0.01-0.01-0.07}$	0.21	0.26	0.55	0.28	9.8	0.31	4.2	1.6
$B_c^+ \to \chi_{c1}\pi^+$	$0.13^{+0.00+0.00+0.00}_{-0.00-0.00-0.00}$	0.2	0.0014	0.068	0.07	0.089	0.021	0.05	0.51
$B_c^+ \to h_c\pi^+$	$0.96^{+0.02+0.02+0.13}_{-0.02-0.02-0.12}$	0.46	0.53	1.1	0.5	16	0.98	6.2	0.54
$B_c^+ \to \chi_{c0}\rho^+$	$1.69^{+0.00+0.02+0.20}_{-0.00-0.02-0.19}$	0.58	0.67	1.3	0.72	33	0.76	–	5.8
$B_c^+ \to \chi_{c1}\rho^+$	$0.43^{+0.01+0.00+0.01}_{-0.01-0.00-0.01}$	0.15	0.1	0.29	0.29	4.6	0.23	1.47	2.8
$B_c^+ \to h_c\rho^+$	$2.42^{+0.04+0.16+0.19}_{-0.04-0.09-0.42}$	1.0	1.3	2.5	1.2	53	2.2	1.24	2.3
$B_c^+ \to \chi_{c0}K^+$	$0.052^{+0.001+0.001+0.006}_{-0.001-0.001-0.006}$	0.016	0.02	0.042	0.0021	–	0.023	0.32	0.12
$B_c^+ \to \chi_{c1}K^+$	$0.010^{+0.000+0.000+0.000}_{-0.000-0.000-0.000}$	0.015	0.00011	0.0051	0.00052	–	0.0016	0.004	0.038
$B_c^+ \to h_cK^+$	$0.075^{+0.001+0.001+0.010}_{-0.001-0.001-0.001}$	0.035	0.041	0.083	0.0038	–	0.074	0.47	0.043
$B_c^+ \to \chi_{c0}K^{*+}$	$0.096^{+0.002+0.001+0.011}_{-0.002-0.001-0.011}$	0.04	0.037	0.07	0.0039	–	0.045	–	0.33
$B_c^+ \to \chi_{c1}K^{*+}$	$0.027^{+0.001+0.000+0.000}_{-0.001-0.000-0.000}$	0.01	0.0073	0.018	0.0018	–	0.017	0.0707	0.18
$B_c^+ \to h_cK^{*+}$	$0.13^{+0.00+0.00+0.02}_{-0.00-0.01-0.01}$	0.07	0.071	0.13	0.0068	–	0.13	0.0618	0.13

predicted by most works have a common property: $Br(B_c \to \chi_{c0}P(V))$ are much larger than $Br(B_c \to \chi_{c1}P(V))$. This characteristic can be tested by the present LHCb experiments.

If replacing $P(V)$ with $D(D^*)$ in the upper decays, the branching ratios of the corresponding decays $B_c \to \chi_{c0(1)}(h_c)D(D^*)$ can be obtained by their decay widths:

$$\Gamma(B_c \to \chi_{c0}D) = \frac{\left(G_F V_{cb}^* V_{cd} m_{B_c}^2\right)^2 \left(1 - r_{\chi_{c0}}^2 - r_D^2\right)}{32\pi m_{B_c}} \times |a_1 f_D F_0^{B_c\chi_{c0}}(m_D^2) + a_2 f_{\chi_{c0}} F_0^{B_cD}(m_{\chi_{c0}}^2)|^2, \quad (96)$$

$$\Gamma(B_c \to \chi_{c0}D^*) = \frac{\left(G_F V_{cb}^* V_{cd} m_{B_c}^2\right)^2 \left(1 - r_{\chi_{c0}}^2 - r_{D^*}^2\right)}{32\pi m_{B_c}} \times |a_1 f_{D^*} F_0^{B_c\chi_{c0}}(m_{D^*}^2) + a_2 f_{\chi_{c0}} A_0^{B_cD^*}(m_{\chi_{c0}}^2)|^2, \quad (97)$$

$$\Gamma(B_c \to \chi_{c1}D) = \frac{\left(G_F V_{cb}^* V_{cd} m_{B_c}^2\right)^2 \left(1 - r_{\chi_{c1}}^2 - r_D^2\right)}{32\pi m_{B_c}} \times |a_1 f_D V_0^{B_c\chi_{c1}}(m_D^2) + a_2 f_{\chi_{c1}} F_0^{B_cD}(m_{\chi_{c1}}^2)|^2. \quad (98)$$

For the decay $B_c \to \chi_{c1}D^*$, the corresponding decay width is the summation of the three polarizations:

$$\Gamma(B_c \to \chi_{c1}D^*) = \frac{|\vec{p}|}{8\pi m_{B_c}^2}\left(|\mathcal{A}_L(B_c \to \chi_{c1}D^*)|^2 + 2\left|\mathcal{A}_N\left(B_c \to \chi_{c1}D^*\right)\right|^2 + 2\left|\mathcal{A}_T\left(B_c \to \chi_{c1}D^*\right)\right|^2\right), \quad (99)$$

Table 12 CLFQM predictions for branching ratios (10^{-3}) of B_c decays to final states containing a P-wave charmonium (χ_{c0}, χ_{c1}, or h_c) and a light pseudoscalar or vector meson. The errors are induced by the same sources as in Table 9

Mode	This work	[78]
$B_c^+ \to \chi_{c0}D^+$	$0.075^{+0.001+0.001+0.001}_{-0.001-0.001-0.001}$	0.033
$B_c^+ \to \chi_{c1}D^+$	$0.019^{+0.000+0.000+0.001}_{-0.000-0.000-0.001}$	0.14×10^{-3}
$B_c^+ \to h_cD^+$	$0.075^{+0.001+0.001+0.011}_{-0.001-0.001-0.010}$	0.066
$B_c^+ \to \chi_{c0}D_s^+$	$2.29^{+0.04+0.02+0.34}_{-0.04-0.07-0.23}$	0.88
$B_c^+ \to \chi_{c1}D_s^+$	$0.60^{+0.01+0.03+0.06}_{-0.01-0.04-0.01}$	0.20×10^{-2}
$B_c^+ \to h_cD_s^+$	$2.24^{+0.04+0.02+0.33}_{-0.04-0.04-0.29}$	1.58
$B_c^+ \to \chi_{c0}D^{*+}$	$0.11^{+0.00+0.00+0.01}_{-0.00-0.00-0.01}$	0.042
$B_c^+ \to \chi_{c1}D^{*+}$	$0.054^{+0.001+0.000+0.000}_{-0.001-0.000-0.000}$	0.026
$B_c^+ \to h_cD^{*+}$	$0.11^{+0.00+0.00+0.03}_{-0.00-0.00-0.01}$	0.071
$B_c^+ \to \chi_{c0}D_s^{*+}$	$2.49^{+0.04+0.02+0.32}_{-0.04-0.33-0.30}$	0.84
$B_c^+ \to \chi_{c1}D_s^{*+}$	$1.23^{+0.02+0.00+0.07}_{-0.02-0.01-0.07}$	0.49
$B_c^+ \to h_cD_s^{*+}$	$2.41^{+0.04+0.02+0.34}_{-0.04-0.02-0.32}$	1.34

where the three polarization amplitudes $\mathcal{A}_L, \mathcal{A}_N, and \mathcal{A}_T$ are given as

$$\mathcal{A}_L(B_c \to \chi_{c1}D^*) = \frac{G_F}{\sqrt{2}} V_{cb}^* V_{cd} m_{B_c}^2 \left\{-(1 - r_{\chi_{c1}}^2 - r_{D^*}^2) \times \left[\frac{a_1 f_{D^*}(1 - r_{\chi_{c1}})}{2r_{\chi_{c1}}} V_1^{B_c\chi_{c1}}(m_{D^*}^2) + \frac{a_2 f_{\chi_{c1}}(1 + r_{D^*})}{2r_{D^*}} A_1^{B_cD^*}(m_{\chi_{c1}}^2)\right] + \frac{a_1\lambda_1 f_{D^*}}{2r_{\chi_{c1}}(1 - r_{\chi_{c1}})} V_2^{B_c\chi_{c1}}(m_{D^*}^2)\right.$$

$$+\frac{a_2\lambda_2 f_{\chi_{c1}}}{2r_{D^*}(1+r_{D^*})}A_2^{B_cD^*}(m_{\chi_{c1}}^2)\Big\}, \tag{100}$$

$$\mathcal{A}_N\left(B_c\to\chi_{c1}D^*\right) = -\frac{G_F}{\sqrt{2}}V_{cb}^*V_{cd}m_{B_c}^2[a_1 f_{D^*}r_{D^*}\left(1-r_{\chi_{c1}}\right)V_1^{B_c\chi_{c1}}\left(m_{D^*}^2\right) + a_2 f_{\chi_{c1}}r_{\chi_{c1}}\left(1+r_{D^*}\right)A_1^{B_cD^*}\left(m_{\chi_{c1}}^2\right)], \tag{101}$$

$$\mathcal{A}_T\left(B_c\to\chi_{c1}D^*\right) = -\frac{G_F}{\sqrt{2}}V_{cb}^*V_{cd}m_{B_c}^2\left[\frac{a_1\sqrt{\lambda_1}}{1-r_{\chi_{c1}}}f_{D^*}r_{D^*}A^{B_c\chi_{c1}}\left(m_{D^*}^2\right) + \frac{a_2\sqrt{\lambda_2}}{1+r_{D^*}}f_{\chi_{c1}}r_{\chi_{c1}}V^{B_cD^*}\left(m_{\chi_{c1}}^2\right)\right], \tag{102}$$

with $\lambda_1=\lambda\left(1,r_{\chi_{c1}}^2,r_{D^*}^2\right),\lambda_2=\lambda\left(1,r_{D^*}^2,r_{\chi_{c1}}^2\right)$. As to the decay widths of the channels $B_c\to\chi_{c0}(\chi_{c1})D_s(D_s^*)$, they can be obtained by performing the replacements $D\to D_s$, $D^*\to D_s^*$, $V_{cd}\to V_{cs}$ in Eqs. (96)–(102). The branching ratios of the these decays are given in Table 12, where we also list the results given by the Salpeter method [78]. This method is the relativistic instantaneous approximation of the original Bethe–Salpeter equation.

Though the $X(3872)$ has been confirmed by many experimental collaborations, such as CDF [80], D0 [81], Babar [82], and LHCb [83], with quantum numbers $J^{PC}=1^{++}$ and isospin $I=0$, there are still many uncertainties. Though many different exotic hadron state interpretations, such as a loosely bound molecular state [84–88], a compact tetraquark state [89–92], $c\bar{c}g$ hybrid meson [93,94], glueball [95], have been put forward, the first raidal excitation of $1P$ charmonium state $\chi_{c1}(1P)$ as the most natural assignment has not been ruled out [96–98]. By assuming the $X(3872)$ as a 1^{++} charmonium state, we calculate the branching ratios of the decays $B_c^+\to X(3872)M$ (here, M represents a light pseudoscalar, a vector meson, or a charmed meson). The analytic expressions of the corresponding decay widths are similar to those of the decays $B_c\to\chi_{c1}M$ listed in Eqs. (91), (92), (98), and (99). In Table 13, we list the branching fractions of the decays $B_c\to X(3872)M$. One can find that our predictions for the decays $B_c^+\to X(3872)\pi^+(K^+)$ are consistent with the results given in the PQCD approach [79], while they are much larger than those calculated in the generalized factorization (GF) approach [30]. Certainly, some of these decays studied using the CLFQM about 15 years ago [14], the differences between our predictions and the previous calculations are induced by taking different values for some parameters.

Lastly, we turn to the branching ratios of the decays with the radially excited S-wave charmonia, such as $\eta_c(2S,3S)$ and $\psi(3S,3S)$, involved in the final states. The correspond decay widths are similar to those of the decays $B_c\to\eta_cM$, $J/\Psi M$, where M represents a light pseudoscalar, a vector meson, or a charmed meson ($D^{(*)}$, $D_s^{(*)}$). As we know, in order to compare with experiments, the ratios

$$R_{\psi(2S)/J/\Psi} \equiv Br(B_c\to\psi(2S)\pi)/Br(B_c\to J/\Psi\pi), \tag{103}$$

$$R_{\eta_c(2S)/\eta_c} \equiv Br(B_c\to\eta_c(2S)\pi)/Br(B_c\to\eta_c\pi), \tag{104}$$

are often used. If we still employ the traditional light-front wave functions for the radially excited charmonia given in Eq. (25), we will get larger branching ratios than most other theoretical predictions; even worse, the obtained value $R_{\psi(2S)/J/\Psi}=0.467$ is much larger than the experimental data $R_{\psi(2S)/J/\Psi}=0.268\pm0.032\pm0.007\pm0.006$ given by PDG [39]. There exists a similar case in Ref. [15], so we follow the same strategy by choosing the modified harmonic oscillator wave functions:

$$\varphi'_{2S}=4\left(\frac{\pi}{\beta'^2}\right)^{\frac{3}{4}}\times\sqrt{\frac{dp'_z}{dx_2}}\exp\left(-\frac{2^\delta}{2}\frac{p_z'^2+p_\perp'^2}{\beta'^2}\right)\left(a_2-b_2\frac{p_z'^2+p_\perp'^2}{\beta'^2}\right), \tag{105}$$

$$\varphi'_{3S}=4\left(\frac{\pi}{\beta'^2}\right)^{\frac{3}{4}}\times\sqrt{\frac{dp'_z}{dx_2}}\exp\left(-\frac{3^\delta}{2}\frac{p_z'^2+p_\perp'^2}{\beta'^2}\right)\left(a_3-b_3\frac{p_z'^2+p_\perp'^2}{\beta'^2}+c_3\frac{(p_z'^2+p_\perp'^2)^2}{\beta'^4}\right). \tag{106}$$

In order to keep the orthogonality and normalization for the wave functions of these radially excited states, one needs to introduce a factor n^δ into the exponential functions in these wave functions, which can be determined by fitting the data of the corresponding decay constants. Similarly, there exists a $1/n$ exponential dependence factor in the wave functions of the hydrogen-like atoms, which are obtained by solving the Schrödinger equation. In Ref. [15], the authors supposed that the parameters shown in Eqs. (105) and (106) are the same as those for $\Upsilon(2S)$ and $\Upsilon(3S)$ under the heavy quark effective theory, which are given as [105]

$$a_2=1.88684,\quad b_2=1.54943,\quad \delta=1/1.82,$$
$$a_3=2.53764,\quad b_3=5.67431,$$
$$c_3=1.85652\quad\text{(scenario I)}. \tag{107}$$

It is noted that these parameters are determined by assuming that the $\Upsilon(iS)(i=2,3)$ mesons have the same β' values as that of β'_Υ for $\Upsilon(1S)$. In fact, under this assumption, once the value of δ is fixed, these parameters given in Eq. (107) can be determined using the orthogonality and normalization for the wave functions of these ground and radially excited

Table 13 CLFQM predictions for branching ratios ($\times 10^{-3}$) of the decays $B_c \to X(3872)M$, where M represents a light pseudoscalar, a vector meson, or a charmed meson. The errors are induced by the same sources as in Table 9

Mode	This work	[14]	[79]	[30]
$B_c^+ \to X(3872)\pi^+$	$0.25^{+0.00+0.01+0.03}_{-0.00-0.01-0.01}$	0.17	0.27	0.06
$B_c^+ \to X(3872)K^+$	$0.020^{+0.000+0.001+0.000}_{-0.000-0.001-0.000}$	0.013	0.025	0.0047
$B_c^+ \to X(3872)\rho^+$	$0.63^{+0.01+0.03+0.03}_{-0.01-0.03-0.08}$	0.41	–	–
$B_c^+ \to X(3872)K^{*+}$	$0.036^{+0.001+0.001+0.004}_{-0.001-0.002-0.002}$	0.024	–	–
$B_c^+ \to X(3872)D^+$	$0.033^{+0.001+0.002+0.001}_{-0.001-0.002-0.000}$	–		
$B_c^+ \to X(3872)D^{*+}$	$0.078^{+0.001+0.007+0.009}_{-0.001-0.007-0.006}$	–		
$B_c^+ \to X(3872)D_s^+$	$1.00^{+0.02+0.15+0.15}_{-0.02-0.15-0.10}$	–		
$B_c^+ \to X(3872)D_s^{*+}$	$1.78^{+0.03+0.07+0.12}_{-0.03-0.07-0.08}$	–		

Table 14 CLFQM predictions for branching ratios ($\times 10^{-4}$) of the decays $B_c \to \psi(2S)P(V)$, $\eta_c(2S)P(V)$ with $P(V)$ representing a light pseudoscalar (vector) meson. For each decay channel, we calculate both in scenario I (upper line) and scenario II (lower line). The first two errors for these entries correspond to the uncertainties from the lifetime and the decay constant of the initial meson B_c, respectively. The last one is from the parameter δ in the modified wave functions of the radially excited charmonium $\psi(2S)$ or $\eta_c(2S)$

Mode	This work	[99]	[100]	[101]	[33]	[66]	[102]	[103]	[15]	[104]	[29]	[58]
$B_c^+ \to \psi(2S)\pi^+$	$4.18^{+0.07+0.02+1.42}_{-0.07-0.02-1.13}$	3.7	1.39	0.63	2.2	2.0	2.66	1.42	2.97	6.7	4.8	1.1
	$2.52^{+0.04+0.01+0.99}_{-0.04-0.01-0.75}$											
$B_c^+ \to \psi(2S)K^+$	$0.33^{+0.01+0.00+0.11}_{-0.01-0.00-0.09}$	0.29	0.109	0.04	0.16	0.089	–	0.102	0.23	–	–	0.1
	$0.20^{+0.01+0.00+0.08}_{-0.01-0.00-0.06}$											
$B_c^+ \to \psi(2S)\rho^+$	$11.93^{+0.21+0.052+4.04}_{-0.21-0.052-3.14}$	11	–	1.6	6.3	4.8	6.83	–	–	–	–	1.8
	$7.18^{+0.13+0.04+2.84}_{-0.13-0.04-2.15}$											
$B_c^+ \to \psi(2S)K^{*+}$	$0.70^{+0.012+0.024+0.21}_{-0.012-0.014-0.20}$	0.57	–	0.081	0.34	0.27	41	–	–	–	–	0.098
	$0.42^{+0.01+0.01+0.15}_{-0.01-0.08-0.13}$											
$B_c^+ \to \eta_c(2S)\pi^+$	$3.35^{+0.06+0.02+1.15}_{-0.06-0.02-0.89}$	2.4	1.44	2.2	2.4	0.66	2.87	1.67	–	10.3	14	1.7
	$0.46^{+0.01+0.01+0.31}_{-0.01-0.01-0.21}$											
$B_c^+ \to \eta_c(2S)K^+$	$0.27^{+0.01+0.00+0.09}_{-0.01-0.00-0.07}$	0.18	0.117	0.16	0.18	0.049	–	0.119	–	–	–	0.1
	$0.036^{+0.001+0.000+0.025}_{-0.001-0.001-0.017}$											
$B_c^+ \to \eta_c(2S)\rho^+$	$8.54^{+0.15+0.04+2.93}_{-0.15-0.05-2.27}$	5.5	12.46	5.25	5.5	1.4	–	0.356	–	–	–	3.6
	$1.17^{+0.02+0.01+0.79}_{-0.02-0.02-0.53}$											
$B_c^+ \to \eta_c(2S)K^{*+}$	$0.49^{+0.01+0.00+0.17}_{-0.01-0.00-0.13}$	0.26	0.239	0.25	0.28	0.0715	–	0.191	–	–	–	0.2
	$0.067^{+0.001+0.001+0.045}_{-0.001-0.001-0.030}$											

states. That is to say, if we only replace β'_Υ with $\beta'_{J/\Psi}$, the values of parameters $a_{2,3}$, $b_{2,3}$, c_3 are not changed. We call this case scenario I (SI). As another possibility, we also assume here that each value of β' in the wave functions of J/Ψ and $\psi(2\,S, 3\,S)$ is different but with $\delta = 1/1.82$ fixed, then we can get another group of values for these parameters:

$$\begin{aligned} &a_2 = 1.99718, \quad b_2 = 1.48536, \quad \delta = 1/1.82, \\ &a_3 = 3.00375, \quad b_3 = 5.54952, \\ &c_3 = 1.49566 \quad \text{(scenario II)}, \end{aligned} \tag{108}$$

which are called scenario II (SII). In this work, we calculate in these two scenarios for the B_c decays with $\psi(2S)$ or $\psi(3S)$ involved in the final states. By using these modified wave functions for $\psi(2S)$, one can obtain that $R_{\psi(2S)/J/\Psi} = 0.212 \pm 0.071$ in SI, which is consistent with the data. At the same time, the tensions between our predictions with other theoretical results are greatly reduced. For example, the branching ratio $Br(B_c^+ \to \eta_c(2\,S)\pi^+) = (7.70^{+0.11+0.03+0.84}_{-0.12-0.04-0.52}) \times 10^{-4}$ using the traditional light-front wave function for $\eta_c(2S)$, while $Br(B_c^+ \to \eta_c(2\,S)\pi^+) = (3.35^{+0.06+0.02+0.89}_{-0.06-0.02-1.20}) \times 10^{-4}$ by replacing with the modified wave function in SI, which are close to the results given by Refs. [33,99,101,102]. This is similar for the decay $B_c^+ \to \psi(2S)\pi^+$. The branching ratios of the decays $B_c^+ \to \eta_c(2\,S)\pi^+$ and $B_c^+ \to \psi(2\,S)\pi^+$ in SI are close to each other; this is also supported by most of the other theoretical predictions shown in Table 14. Furthermore, the differences of the branching ratios of the decays $B_c \to J/\Psi(2S)P(V)$

between these two scenarios are not large, while they are very different for the decays with $\eta_c(2S)$ involved. So one can use the decay channels $B_c \to \eta_c(2S)P(V)$ to check which scenario is more accurate by comparing with the future experimental data.

In Table 15, we calculate the branching ratios of the decays $B_c \to \psi(2S)D_{(s)}(D^*_{(s)})$, $\eta_c(2S)D_{(s)}(D^*_{(s)})$. From our calculations and the numerical results, we find the following points:

1. The branching ratios of the decays with $\eta_c(2S)$ involved are more sensitive to the shape parameter β'. For example, for the decays $B_c^+ \to \eta_c(2S)D^+_{(s)}$, $\eta_c(2S)D^{*+}_{(s)}$, their branching ratios in SI are about five times larger than those in SII, while for the decays $B_c^+ \to \psi(2S)D^+_{(s)}$, $\psi(2S)D^{*+}_{(s)}$, the differences of the results between these two scenarios are less than two times.
2. The branching ratios of the decays with D_s^+ or D_s^{*+} involved are at least one order larger than those of the corresponding decays with D^+ or D^{*+} involved. It is because the former (the latter) are suppressed (enhanced) by the CKM matrix elements.
3. On the whole, the predictions in SII are closer to other theoretical results than those in SI, which supports that taking a different value of the shape parameter β' for each radially excited charmonium is more reasonable.

At present, only a few papers have studied B_c decays with $\psi(3S)$ or $\eta_c(3S)$ involved, which are listed in Tables 16 and 17. Most theoretical predictions show that the branching ratios of these decays are about or less than 10^{-4}. Meanwhile, for the decay $B_c^+ \to \eta_c(3S)\pi^+$, its branching ratio was predicted as 1.4×10^{-3} in the PQCD approach [29], where the authors obtained that the branching ratios of the decays $B_c \to \eta_c(2S)\pi^+$ and $B_c^+ \to \eta_c(3S)\pi^+$ are almost equivalent. Our prediction for the branching ratio of the decay $B_c^+ \to \eta_c(2S)\pi^+$ is about 2.5 times larger than that of $B_c^+ \to \eta_c(3S)\pi^+$ in SI. Certainly, the difference between $Br(B_c^+ \to \eta_c(2S)\pi^+)$ and $Br(B_c^+ \to \eta_c(3S)\pi^+)$ in SII is more than one order. There exists a similar relation between the decays $B_c^+ \to \psi(2S)\pi^+$ and $B_c^+ \to \psi(3S)\pi^+$. So we suggest that the ratios $Br(B_c^+ \to \eta_c(2S)\pi^+)/Br(B_c^+ \to \eta_c(3S)\pi^+)$ and $Br(B_c^+ \to \psi(2S)\pi^+)/Br(B_c^+ \to \psi(3S)\pi^+)$ can be measured by LHCb experiments to distinguish which shape parameters for these radially excited charmonia are more appropriate. In Ref. [106], the authors calculated the branching ratios of these decays by using the improved Bethe–Salpeter method. Their results of the decays $B_c \to \psi(3S)P(V)$, where $P(V)$ represents a light pseudoscalar (vector) meson, agree with our predictions in SI within errors. Meanwhile, there exist larger divergences for the branching ratios of the decays $B_c \to \eta_c(3S)P(V)$ with other theoretical results. The relativistic independent quark model (RIQM) based on a flavor-independent interaction potential was used in Ref. [100], where two groups of results corresponding to two sets of Wilson coefficients were obtained.

If replacing $P(V)$ with $D_{(s)}(D^*_{(s)})$, we can study the branching ratios for the decays $B_c \to \psi(3S)D_{(s)}(D^*_{(s)})$, $\eta_c(3S)D_{(s)}(D^*_{(s)})$, which are listed in Table 17. Just as in the case of the decays $B_c \to \psi(2S)D_{(s)}(D^*_{(s)})$, $\eta_c(2S)D_{(s)}(D^*_{(s)})$, the branching ratios of the decays with $D_s^{(*)}$ involved are much larger than those of the decays with $D^{(*)}$ involved because of the CKM factors. In addition to the RIQ model, some of these decays are also researched by using the improved Bethe–Salpeter method [103], where the branching ratios of the decays $B_c \to \psi(3S)D^{*+}$, $\eta_c(3S)D_s^{*+}$ are consistent with our predictions in SI. Whereas, the branching ratio of the decay $B_c^+ \to \psi(3S)D^+$ is predicted as 3.62×10^{-8} and much smaller than our result. We predict that some of the decays with $\eta_c(3S)$ or $\psi(3S)$ involved, such as $B_c \to \eta_c(3S)\rho$, $B_c \to \psi(3S)D_s^*$, might have larger branching ratios (up to 10^{-4}) and may be accessible at the High-Luminosity Large Hadron Collider in the near future.

Comparing Tables 9, 14, and 16, one can find that there is a hierarchy for these decays:

$$Br(B_c \to J/\Psi P(V)) > Br(B_c \to \psi(2S)P(V)) > Br(B_c \to \psi(3S)P(V)), \quad (109)$$

$$Br(B_c \to \eta_c P(V)) > Br(B_c \to \eta_c(2S)P(V)) > Br(B_c \to \eta_c(3S)P(V)), \quad (110)$$

where $P(V)$ represents a light pseudoscalar (vector) meson. This is because for the decays with the higher excited charmonia involved, the phase spaces are tighter, and the form factors are smaller and less sensitive to the change of the momentum transfer q^2.

4 Summary

In this work, we study the form factors of B_c decays into charmonia in the covariant light-front quark model. Here, the charmonia refer to the S-wave mesons, such as J/Ψ, η_c, the corresponding radially excited states, such as $\psi(2S, 3S)$, $\eta_c(2S, 3S)$, and the P-wave mesons, such as χ_{c0}, χ_{c1}, h_c and $X(3872)$. Certainly, the form factors of the $B_c \to D^{(*)}$, $D_s^{(*)}$ transitions are also considered for the purpose of the branching ratio calculation. We find that the analytical expressions for $B_c \to S, A$ transition form factors can be obtained from those of $B_c \to P, V$ analytical expressions by some simple replacements. The form factor $F^{B_c\eta_c}(V^{B_cJ/\Psi})$ has been calculated by many approaches, most results of which lie in the range of $0.5 \sim 0.7(0.5 \sim 1.0)$. We obtain a moderate value of $F^{B_c\eta_c} = 0.6(V^{B_cJ/\Psi} = 0.76)$. This can be used to check which method is more

Table 15 CLFQM predictions for branching ratios ($\times 10^{-4}$) of the decays $B_c \to \psi(2S)D_{(s)}^{+}(D_{(s)}^{*+})$, $\eta_c(2S)D_{(s)}^{+}(D_{(s)}^{*+})$. For each decay channel, we calculate in SI (upper line) and SII (lower line). The errors for these entries are the same as those in Table 14

Mode	This work	[103]	[15]	[99]	[66]	[100]	[33]
$B_c^+ \to \psi(2S)D^+$	$0.71^{+0.01+0.00+0.23}_{-0.01-0.00-0.18}$	0.0156	0.138	0.24	0.073	0.07(0.11)	0.11
	$0.44^{+0.00+0.00+0.17}_{-0.00-0.00-0.13}$						
$B_c^+ \to \psi(2S)D^{*+}$	$0.92^{+0.16+0.05+0.27}_{-0.16-0.01-0.21}$	1.29	0.42	–	0.052	–	–
	$0.61^{+0.01+0.00+0.20}_{-0.01-0.00-0.16}$						
$B_c^+ \to \psi(2S)D_s^+$	$10.92^{+0.19+1.07+2.67}_{-0.19-0.97-3.85}$	2.69	3.08	5.25	1.2	2.57(3.94)	4.4
	$6.67^{+0.12+0.84+1.79}_{-0.12-0.75-2.71}$						
$B_c^+ \to \psi(2S)D_s^{*+}$	$19.25^{+0.33+0.21+6.16}_{-0.33-0.32-4.36}$	27.2	8.85	–	1.7	–	–
	$12.60^{+0.22+0.16+4.53}_{-0.22-0.27-3.12}$						
$B_c^+ \to \eta_c(2S)D^+$	$0.35^{+0.01+0.00+0.11}_{-0.01-0.00-0.10}$	0.0364	–	0.057	0.022	0.161(0.21)	0.2
	$0.079^{+0.001+0.001+0.037}_{-0.001-0.001-0.027}$						
$B_c^+ \to \eta_c(2S)D^{*+}$	$0.50^{+0.01+0.00+0.15}_{-0.01-0.00-0.11}$	0.292	–	0.21	0.00078	0.12(0.185)	0.11
	$0.13^{+0.00+0.00+0.05}_{-0.00-0.00-0.04}$						
$B_c^+ \to \eta_c(2S)D_s^+$	$10.62^{+0.19+0.67+0.87}_{-0.19-0.81-1.89}$	4.46	–	0.67	0.785	5.81(7.4)	8.7
	$2.36^{+0.04+0.52+0.62}_{-0.04-0.60-0.34}$						
$B_c^+ \to \eta_c(2S)D_s^{*+}$	$11.07^{+0.20+0.17+3.62}_{-0.20-0.28-2.45}$	3.56	–	4.5	0.2	4.61(6.13)	4.4
	$2.76^{+0.05+0.08+1.34}_{-0.05-0.14-0.79}$						

Table 16 CLFQM predictions for branching ratios ($\times 10^{-5}$) of the decays $B_c \to \psi(3S)P(V)$, $\eta_c(3S)P(V)$, with $P(V)$ representing a light pseudoscalar (vector) meson. For each decay channel, we calculate both in SI (upper line) and SII (lower line). The errors for these entries are the same as those in Table 14

Mode	This work	[100]	[106]	[29]
$B_c^+ \to \psi(3S)\pi^+$	$16.15^{+0.29+0.06+17.14}_{-0.29-0.07-8.72}$	4.7(4.8)	3.11	48
	$1.80^{+0.03+0.00+3.30}_{-0.03-0.00-1.29}$			
$B_c^+ \to \psi(3S)K^+$	$1.28^{+0.02+0.01+1.36}_{-0.02-0.01-0.69}$	0.35(0.36)	0.214	–
	$0.14^{+0.00+0.00+0.26}_{-0.00-0.00-0.10}$			
$B_c^+ \to \psi(3S)\rho^+$	$46.47^{+0.82+0.27+49.03}_{-0.82-0.66-24.91}$	–	3.35	–
	$5.15^{+4.48+0.02+9.57}_{-4.48-0.04-3.71}$			
$B_c^+ \to \psi(3S)K^{*+}$	$2.78^{+0.05+0.04+2.87}_{-0.05-0.02-1.51}$	–	0.229	–
	$0.31^{+0.01+0.00+0.56}_{-0.01-0.00-0.22}$			
$B_c^+ \to \eta_c(3S)\pi^+$	$13.50^{+0.24+0.06+14.31}_{-0.24-0.06-7.29}$	4.7(4.8)	2.16	140
	$0.29^{+0.01+0.00+1.14}_{-0.01-0.00-0.29}$			
$B_c^+ \to \eta_c(3S)K^+$	$1.07^{+0.02+0.00+1.13}_{-0.02-0.01-0.58}$	0.38(0.39)	0.153	–
	$0.024^{+0.000+0.000+0.090}_{-0.000-0.000-0.023}$			
$B_c^+ \to \eta_c(3S)\rho^+$	$34.36^{+0.61+0.15+36.42}_{-0.61-0.16-18.57}$	14.9(15.5)	4.29	–
	$0.76^{+0.01+0.01+2.91}_{-0.01-0.01-0.73}$			
$B_c^+ \to \eta_c(3S)K^{*+}$	$1.97^{+0.04+0.01+2.08}_{-0.04-0.01-1.06}$	0.79(0.81)	0.225	–
	$0.044^{+0.001+0.000+0.017}_{-0.001-0.000-0.042}$			

favored by comparing to the future experimental data. Compared with the form factors of B_c transitions to these two ground-state S-wave charmonia, those of B_c transitions to the radially excited S-wave charmonia, P-wave charmonia, and charmed mesons are smaller. Except for each form factor at the zero recoiling point, we also calculate the corresponding one at the maximally recoiling point. Furthermore, we plot the q^2 dependence for each transition form factor. Then we calculate the branching ratios of 80 B_c decays with a charmonium involved in each channel. We find that the decays $B_c^+ \to J/\Psi(\eta_c)\pi^+(\rho^+)$ and $B_c^+ \to J/\Psi(\eta_c)D_s^+(D_s^{*+})$ have larger branching ratios, which can reach the order of 10^{-3}, while most other decay channels have smaller branching ratios, which are suppressed by $1 \sim 3$ orders. These

Table 17 CLFQM predictions for branching ratios ($\times 10^{-5}$) of the decays $B_c^+ \to \psi(3S) D_{(s)}^+ (D_{(s)}^{*+})$, $\eta_c(3S) D_{(s)}^+ (D_{(s)}^{*+})$. For each decay channel, we calculate in scenario I (upper line) and scenario II (lower line). The errors for these entries are the same as those in Table 14

Mode	This work	[100]	[103]
$B_c^+ \to \psi(3S) D^+$	$1.68^{+0.03+0.06+1.57}_{-0.03-0.05-0.89}$	0.02(0.092)	3.62×10^{-3}
	$0.25^{+0.01+0.02+0.33}_{-0.01-0.02-0.17}$		
$B_c^+ \to \psi(3S) D^{*+}$	$2.78^{+0.05+0.01+2.61}_{-0.05-0.00-1.36}$	–	3.38
	$0.47^{+0.01+0.00+0.60}_{-0.01-0.00-0.27}$		
$B_c^+ \to \psi(3S) D_s^+$	$50.58^{+0.89+16.39+50.71}_{-0.89-16.54-24.73}$	6.6(7.9)	3.76
	$7.74^{+0.14+0.96+4.44}_{-0.14-0.89-1.16}$		
$B_c^+ \to \psi(3S) D_s^{*+}$	$58.38^{+1.03+1.11+54.11}_{-1.03-0.98-29.92}$	–	58.9
	$9.42^{+0.17+0.42+2.13}_{-0.17-0.44-5.89}$		
$B_c^+ \to \eta_c(3S) D^+$	$1.35^{+0.02+0.06+1.18}_{-0.02-0.05-0.70}$	0.21(0.36)	–
	$0.095^{+0.002+0.015+0.133}_{-0.002-0.013-0.071}$		
$B_c^+ \to \eta_c(3S) D^{*+}$	$1.95^{+0.03+0.00+1.74}_{-0.03-0.01-0.92}$	0.032(0.09)	–
	$0.18^{+0.00+0.00+0.24}_{-0.00-0.00-0.10}$		
$B_c^+ \to \eta_c(3S) D_s^+$	$41.11^{+0.73+1.98+2.87}_{-0.73-2.39-18.31}$	7.72(11.5)	–
	$3.33^{+0.06+0.61+0.85}_{-0.06-0.68-1.66}$		
$B_c^+ \to \eta_c(3S) D_s^{*+}$	$43.19^{+0.76+1.05+37.26}_{-0.76-0.89-21.37}$	3.2(4.6)	–
	$3.83^{+0.07+0.28+4.90}_{-0.07-0.29-2.47}$		

predictions will be tested in the future by the LHCb experiments.

Acknowledgements This work is partly supported by the National Natural Science Foundation of China under grant no. 11347030, the Program of Science and Technology Innovation Talents in Universities of Henan Province 14HASTIT037, and the Natural Science Foundation of Henan Province under grant no. 232300420116. Z. Q. Zhang would like to thank Prof. Hai-Yang Cheng, Chun-Khiang Chua, Hong-Wei Ke, and Hsiang-nan Li for helpful discussions.

Data Availability Statement This manuscript has no associated data or the data will not be deposited. [Authors' comment: This work is a theoretical study. No relevant data to deposit.]

Funded by SCOAP[3]. SCOAP[3] supports the goals of the International Year of Basic Sciences for Sustainable Development.

Appendix A: Some specific rules under the p^- integration

When preforming the integration, we need to include the zero-mode contribution. It amounts to performing the integration in a proper way in the CLFQM. Specifically, we use the following rules given in Refs. [10,11]:

$$\hat{p}'_{1\mu} \doteq P_\mu A_1^{(1)} + q_\mu A_2^{(1)}, \tag{A1}$$

$$\hat{p}'_{1\mu}\hat{p}'_{1\nu} \doteq g_{\mu\nu} A_1^{(2)} + P_\mu P_\nu A_2^{(2)} + \left(P_\mu q_\nu + q_\mu P_\nu\right) A_3^{(2)} + q_\mu q_\nu A_4^{(2)}, \tag{A2}$$

$$Z_2 = \hat{N}'_1 + m_1'^2 - m_2^2 + (1-2x_1)\, M'^2 + \left(q^2 + q\cdot P\right) \frac{p'_\perp \cdot q_\perp}{q^2}, \tag{A3}$$

$$A_1^{(1)} = \frac{x_1}{2}, \quad A_2^{(1)} = A_1^{(1)} - \frac{p'_\perp \cdot q_\perp}{q^2},$$

$$A_3^{(2)} = A_1^{(1)} A_2^{(1)}, \tag{A4}$$

$$A_4^{(2)} = \left(A_2^{(1)}\right)^2 - \frac{1}{q^2} A_1^{(2)}, \quad A_1^{(2)} = -p_\perp'^2 - \frac{\left(p'_\perp \cdot q_\perp\right)^2}{q^2},$$

$$A_2^{(2)} = \left(A_1^{(1)}\right)^2. \tag{A5}$$

References

1. M. V. Terent'ev, Light Front Dynamics and Nucleons from Relativistic Quarks, Sov. J. Phys. **24**, 106 (1976) (V.B. Berestetsky and M.V. Terent'ev, Erratum ibid. **24**, 547 (1976); Erratum ibid. 25, 347 (1977))
2. P.L. Chung, F. Coester, W.N. Polyzou, Charge form factors of quark-model pions. Phys. Lett. B. **205**, 545 (1988)
3. P.A.M. Dirac, Forms of relativistic dynamics. Rev. Mod. Phys. **21**, 392 (1949)
4. S.J. Brodsky, H.C. Pauli, S.S. Pinsky, Quantum chromodynamics and other field theories on the light cone. Phys. Rep. **301**, 299 (1998). arXiv:hep-ph/9705477

5. W. Jaus, Semileptonic decays of B and D mesons in the light-front formalism. Phys. Rev. D **41**, 3394 (1990)
6. W. Jaus, Relativistic constituent-quark model of electroweak properties of light mesons. Phys. Rev. D **44**, 2851 (1991)
7. C.R. Ji, P.L. Chung, S.R. Cotanch, Light-cone quark-model axial-vector-meson wave function. Phys. Rev. D **45**, 4214 (1992)
8. H.Y. Cheng, C.Y. Cheung, C.W. Hwang, Mesonic form factors and the Isgur–Wise function on the light-front. Phys. Rev. D **55**, 1559 (1997). arXiv:hep-ph/9607332
9. H.Y. Cheng, C.Y. Cheung, C.W. Hwang, W.M. Zhang, A covariant light front model of heavy mesons within HQET. Phys. Rev. D **57**, 5598 (1998). arXiv:hep-ph/9709412
10. W. Jaus, Covariant analysis of the light-front quark model. Phys. Rev. D **60**, 054026 (1999)
11. H.Y. Cheng, C.K. Chua, C.W. Hwang, Covariant light-front approach for s-wave and p-wave mesons: its application to decay constants and form factors. Phys. Rev. D **69**, 074025 (2004). arXiv:hep-ph/0310359
12. W. Wang, Y.L. Shen, C.D. Lu, Covariant light-front approach for B_c transition form factors. Phys. Rev. D **79**, 054012 (2009). arXiv:0811.3748 [hep-ph]
13. X.X. Wang, W. Wang, C.D. Lu, B_c to P-wave charmonia transitions in covariant light-front approach. Phys. Rev. D **79**, 114018 (2009). arXiv:0901.1934 [hep-ph]
14. W. Wang, Y.L. Shen, C.D. Lu, The study of $B_c^- \to X(3872)\pi^-(K^-)$ decays in the covariant light-front approach. Eur. Phys. J. C **51**, 841 (2007). arXiv:0704.2493 [hep-ph]
15. H.W. Ke, T. Liu, X.Q. Li, Transitions of $B_c \to \psi(1S, 2S)$ and the modified harmonic oscillator wave function in LFQM. Phys. Rev. D **89**, 017501 (2014). arXiv:1307.5925 [hep-ph]
16. H.M. Choi, C.R. Ji, Self-consistent covariant description of vector meson decay constants and chirality-even quark–antiquark distribution amplitudes up to twist-3 in the light-front quark model. Phys. Rev. D **89**, 033011 (2014). arXiv:1308.4455 [hep-ph]
17. Q. Chang, X.N. Li, X.Q. Li, F. Su, Y.D. Yang, Self-consistency and covariance of light-front quark models: testing via P, V and A meson decay constants, and $P \to P$ weak transition form factors. Phys. Rev. D **98**, 114018 (2018). arXiv:1810.00296 [hep-ph]
18. Q. Chang, X.L. Wang, L.T. Wang, Tensor form factors of $P \to P$, S, V and A transitions within standard and covariant light-front approaches. Chin. Phys. C **44**, 083105 (2020). arXiv:2003.10833 [hep-ph]
19. L. Chen, Y.W. Ren, L.T. Wang, Q. Chang, Form factors of $P \to T$ transition within the light-front quark models. Eur. Phys. J. C **82**, 451 (2022). arXiv:2112.08016 [hep-ph]
20. I.P. Gouz, V.V. Kiselev, A.K. Likhoded, V.I. Romanovsky, O.P. Yushchenko, Prospects for the B_c studies at LHCb. Phys. Atom. Nucl. **67**, 1559 (2004). arXiv:hep-ph/0211432
21. R. Aaij et al., [LHCb collaboration], First observation of the decay $B_c^+ \to J/\Psi\pi^+\pi^-\pi^+$. Phys. Rev. Lett. **108**, 251802 (2012). arXiv:1204.0079 [hep-ex]
22. R. Aaij et al., [LHCb collaboration], Measurements of B_c^+ production and mass with the $B_c^+ \to J/\Psi\pi^+$ decay. Phys. Rev. Lett. **109**, 232001 (2012). arXiv:1209.5634 [hep-ex]
23. R. Aaij et al., [LHCb collaboration], First observation of the decay $B_c^+ \to J/\Psi K^+$. JHEP **09**, 075 (2013). arXiv:1306.6723 [hep-ex]
24. R. Aaij et al., [LHCb collaboration], Observation of $B_c^+ \to J/\Psi D_s^+$ and $B_c^+ \to J/\Psi D_s^{*+}$ decays. Phys. Rev. D **87**, 112012 (2013). arXiv:1304.4530 [hep-ex]
25. R. Aaij et al., [LHCb collaboration], Observation of the decay $B_c \to J/\Psi K^+K^-\pi^+$. JHEP **11**, 094 (2013). arXiv:1309.0587 [hep-ex]
26. R. Aaij et al., [LHCb collaboration], Observation of the Decay $B_c^+ \to B_s^0\pi^+$. Phys. Rev. Lett. **111**, 181801 (2013). arXiv:1308.4544 [hep-ex]
27. Y. N. Gao, J. B. He, R. Patrick, S. Marie-hélène, and Z. W. Yang, Experimental Prospects of the B_c Studies of the LHCb Experiment, Chin. Phys. Lett. **27**, 061302 (2010)
28. Z. Rui, Probing the P-wave charmonium decays of B_c meson. Phys. Rev. D **97**, 033001 (2018). arXiv:1712.08928 [hep-ph]
29. Z. Rui, H. Li, G.X. Wang, Y. Xiao, Semileptonic decays of B_c meson to S-wave charmonium states in the perturbative QCD approach. Eur. Phys. J. C **76**, 564 (2016). arXiv:1602.08918 [hep-ph]
30. Y.K. Hsiao, C.Q. Geng, Branching fractions of $B_{(c)}$ decays involving J/ψ and $X(3872)$. Chin. Phys. C **41**, 013101 (2017). arXiv:1607.02718 [hep-ph]
31. Q. Chang, L.L. Chen, S. Xu, Study of $B_c \to J/\psi V$ and $B_c^* \to \eta_c V$ decays within the QCD factorization. J. Phys. G **45**, 075005 (2018). arXiv:1806.02076 [hep-ph]
32. V.V. Kiselev, A.E. Kovalsky, A.K. Likhoded, B_c decays and lifetime in QCD sum rules. Nucl. Phys. B **585**, 353 (2000). arXiv:hep-ph/0002127
33. C.H. Chang, Y.Q. Chen, Decays of the B_c meson. Phys. Rev. D **49**, 3399 (1994)
34. M.A. Ivanov, J.G. Korner, P. Santorelli, Exclusive semileptonic and nonleptonic decays of the B_c meson. Phys. Rev. D **73**, 054024 (2006). arXiv:hep-ph/0602050
35. R.N. Faustov, V.O. Galkin, X.W. Kang, Phys. Rev. D **106**, 013004 (2022). arXiv:2206.10277 [hep-ph]
36. C.F. Qiao, P. Sun, D. Yang, R.L. Zhu, B_c exclusive decays to charmonium and a light meson at next-to-leading order accuracy. Phys. Rev. D **89**, 034008 (2014). arXiv:1209.5859 [hep-ph]
37. M. Wirbel, B. Stech, M. Bauer, Exclusive semileptonic decays of heavy mesons. Z. Phys. C **29**, 637 (1985)
38. T.W. Chiu et al., [TWQCD], Beauty mesons in lattice QCD with exact chiral symmetry. Phys. Lett. B **651**, 171 (2007). arXiv:0705.2797 [hep-ph]
39. R. L. Workman et al., [Particle Data Group], Review of Particle Physics. PTEP **2022**, 083C01 (2022)
40. D. Bečirević, G. Duplančić, B. Klajn, B. Melić, F. Sanfilippo, Lattice QCD and QCD sum rule determination of the decay constants of η_c, J/Ψ and h_c states. Nucl. Phys. B **883**, 306 (2014). arXiv:1312.2858 [hep-ph]
41. Y.M. Wang, C.D. Lu, Weak productions of new charmonium in semi-leptonic decays of B_c. Phys. Rev. D **77**, 054003 (2008). arXiv:0707.4439 [hep-ph]
42. Z.Z. Song, C. Meng, K.T. Chao, $B \to \eta_c K(\eta_c' K)$ decays in QCD factorization. Eur. Phys. J. C **36**, 365 (2004). arXiv:hep-ph/0209257
43. M.A. Olpak, A. Ozpineci, V. Tanriverdi, Light cone distribution amplitudes of excited P-wave heavy quarkonia at the leading twist. Phys. Rev. D **96**, 014026 (2017). arXiv:1608.04539 [hep-ph]
44. D. Becirevic, P. Boucaud, J.P. Leroy, V. Lubicz, G. Martinelli, F. Mescia, F. Rapuano, Non-perturbatively improved heavy-light mesons: masses and decay constants. Phys. Rev. D **60**, 074501 (1999). arXiv:hep-lat/9811003
45. M.A. Nobes, R.M. Woloshyn, Decays of the B_c meson in a relativistic quark meson model. J. Phys. G **26**, 1079 (2000). arXiv:hep-ph/0005056
46. M.A. Ivanov, J.G. Korner, P. Santorelli, Semileptonic decays of B_c mesons into charmonium states in a relativistic quark model. Phys. Rev. D **71**, 094006 (2005) (Erratum ibid. Phys. Rev. D 75, 019901 (2007)). arXiv:hep-ph/0501051
47. J.F. Sun, D.S. Du, Y.L. Yang, Study of $B_c \to J/\Psi\pi, \eta_c\pi$ decays with perturbative QCD approach. Eur. Phys. J. C **60**, 107 (2009). arXiv:0808.3619 [hep-ph]
48. R. Dhir, N. Sharma, R.C. Verma, Flavor dependence of B_c meson form factors and $B_c \to PP$ decays. J. Phys. G **35**, 085002 (2008)
49. R.C. Verma, A. Sharma, Quark diagram analysis of weak hadronic decays of the B_c^+ meson. Phys. Rev. D **65**, 114007 (2002)

50. R. Dhir, R.C. Verma, B_c meson form factors and $B_c \to PV$ decays involving flavor dependence of transverse quark momentum. Phys. Rev. D **79**, 034004 (2009). arXiv:0810.4284 [hep-ph]
51. V.V. Kiselev, A.K. Likhoded, A.I. Onishchenko, Semileptonic B_c meson decays in sum rules of QCD and NRQCD. Nucl. Phys. B **569**, 473 (2000). arXiv:hep-ph/9905359
52. M.A. Ivanov, J.G. Korner, P. Santorelli, The semileptonic decays of the B_c meson. Phys. Rev. D **63**, 074010 (2001). arXiv:hep-ph/0007169
53. F. Zuo, T. Huang, $B_c(B) \to D\ell\bar{\nu}$ form factors in light-cone sum rules and the D-meson distribution amplitude. Chin. Phys. Lett. **24**, 61 (2007). arXiv:hep-ph/0611113
54. T. Huang, F. Zuo, Semileptonic B_c decays and charmonium distribution amplitude. Eur. Phys. J. C **51**, 833 (2007). arXiv:hep-ph/0702147
55. V.V. Kiselev, A.E. Kovalsky, A.K. Likhoded, B_c decays and lifetime in QCD sum rules. Nucl. Phys. B **585**, 353 (2000). arXiv:hep-ph/0002127
56. V.V. Kiselev, Exclusive decays and lifetime of B_c meson in QCD sum rules. arXiv:hep-ph/0211021
57. D.S. Du, Z. Wang, Predictions of the standard model for $B_c^{\pm}$ weak decays. Phys. Rev. D **39**, 1342 (1989)
58. D. Ebert, R.N. Faustov, V.O. Galkin, Weak decays of the B_c meson to charmonium and D mesons in the relativistic quark model. Phys. Rev. D **68**, 094020 (2003). arXiv:hep-ph/0306306
59. E. Hernandez, J. Nieves, J.M. Verde-Velasco, Study of exclusive semileptonic and non-leptonic decays of B_c^- in a non-relativistic quark model. Phys. Rev. D **74**, 074008 (2006). arXiv:hep-ph/0607150
60. P. Colangelo, G. Nardulli, N. Paver, QCD sum rules and B decays. arXiv:hep-ph/9303220
61. V.V. Kiselev, A.V. Tkabladze, Semileptonic B_c decays from QCD sum rules. Phys. Rev. D **48**, 5208 (1993)
62. G. Buchalla, A.J. Buras, M.E. Lautenbacher, Weak decays beyond leading logarithms. Rev. Mod. Phys. **68**, 1125 (1996). arXiv:hep-ph/9512380
63. D. Ebert, R.N. Faustov, V.O. Galkin, Weak decays of the B_c meson to charmonium and D mesons in the relativistic quark model. Phys. Rev. D **68**, 094020 (2003). arXiv:hep-ph/0306306
64. S. Naimuddin, S. Kar, M. Priyadarsini, N. Barik, P.C. Dash, Non-leptonic two-body B_c meson decays. Phys. Rev. D **86**, 094028 (2012)
65. S. Kar, P.C. Dash, M. Priyadarsini, S. Naimuddin, N. Barik, Non-leptonic $B_c \to VV$ decays. Phys. Rev. D **88**, 094014 (2013)
66. P. Colangelo, F. De Fazio, Using heavy quark spin symmetry in semileptonic B_c decays. Phys. Rev. D **61**, 034012 (2000). arXiv:hep-ph/9909423
67. A.A. El-Hady, J.H. Munoz, J.P. Vary, Semileptonic and nonleptonic B_c decays. Phys. Rev. D **62**, 014019 (2000). arXiv:hep-ph/9909406
68. Z. Rui, Z.T. Zou, S-wave ground state charmonium decays of B_c mesons in the perturbative QCD approach. Phys. Rev. D **90**, 114030 (2014). arXiv:1407.5550 [hep-ph]
69. R. Aaij et al., [LHCb collaboration], Measurement of the ratio of branching fractions $mathcal B(B_c^+ \to J/\Psi K^+)/mathcal B(B_c^+ \to J/\Psi\pi^+)$. JHEP **09**, 153 (2016). arXiv:1607.06823 [hep-ph]
70. H.F. Fu, Y. Jiang, C.S. Kim, G.L. Wang, Probing non-leptonic two-body decays of B_c meson. JHEP **06**, 015 (2011). arXiv:1102.5399 [hep-ph]
71. G. Aad et al., [ATLAS collaboration], Study of $B_c^+ \to J/\Psi D_s^+$ and $B_c^+ \to J/\Psi D_s^{*+}$ decays in pp collisions at $\sqrt{s} =$ 13 TeV with the ATLAS detector. JHEP **08**, 087 (2022). arXiv:2203.01808 [hep-ph]
72. D. Ebert, R.N. Faustov, V.O. Galkin, Semileptonic and nonleptonic decays of B_c mesons to orbitally excited heavy mesons in the relativistic quark model. Phys. Rev. D **82**, 034019 (2010). arXiv:1007.1369 [hep-ph]
73. M.A. Ivanov, J.G. Korner, P. Santorelli, Exclusive semileptonic and nonleptonic decays of the B_c meson. Phys. Rev. D **73**, 054024 (2006). arXiv:hep-ph/0602050
74. C.H. Chang, Y.Q. Chen, G.L. Wang, H.S. Zong, Decays of the meson B_c to a P wave charmonium state χ_c or h_c. Phys. Rev. D **65**, 014017 (2002). arXiv:hep-ph/0103036
75. V.V. Kiselev, O.N. Pakhomova, V.A. Saleev, Two particle decays of B_c meson into charmonium states. J. Phys. G **28**, 595 (2002). arXiv:hep-ph/0110180
76. Z.H. Wang, G.L. Wang, C.H. Chang, The B_c decays to P-wave charmonium by improved Bethe–Salpeter approach. J. Phys. G **39**, 015009 (2012). arXiv:1107.0474 [hep-ph]
77. Z. Rui, Probing the P-wave charmonium decays of B_c meson. Phys. Rev. D **97**, 033001 (2018). arXiv:1712.08928 [hep-ph]
78. H.F. Fu, Y. Jiang, C.S. Kim, G.L. Wang, Probing non-leptonic two-body decays of B_c meson. JHEP **06**, 015 (2011). arXiv:1102.5399 [hep-ph]
79. Z.Q. Zhang, Z.L. Guan, Y.C. Zhao, Z.Y. Zhang, Z.J. Sun, N. Wang, X.D. Ren, Insights into the nature of the $X(3872)$ through B meson decays. Chin. Phys. C **47**, 013103 (2023). arXiv:2208.07990 [hep-ph]
80. D. Acosta et al., [CDF II collaboration], Observation of the Narrow State $X(3872) \to J/\Psi\pi^+\pi^-$ in $\bar{p}p$ Collisions at $\sqrt{s} = 1.96TeV$. Phys. Rev. Lett. **93**, 072001 (2004). arXiv:hep-ex/0312021
81. V. M. Abazov et al., [D0 collaboration], Observation and properties of the $X(3872)$ decaying to $J/\Psi\pi^+\pi^-$ in $p\bar{p}$ collisions at $\sqrt{s} = 1.96TeV$. Phys. Rev. Lett. **93**, 162002 (2004). arXiv:hep-ex/0405004
82. B. Aubert et al., [BaBar collaboration], Study of the $B^- \to J/\Psi K^-\pi^+\pi^-$ decay and measurement of the $B^- \to X(3872)K^-$ branching fraction. Phys. Rev. D **71**, 071103 (2005). arXiv:hep-ex/0406022
83. R. Aaij et al., [LHCb collaboration], Study of the lineshape of the $\chi_{c1}(3872)$ state. Phys. Rev. D **102**, 092005 (2020). arXiv:2005.13419 [hep-ph]
84. F.E. Close, P.R. Page, The $D^{*0}\bar{D}^0$ threshold resonance. Phys. Lett. B **578**, 119 (2004). arXiv:hep-ph/0309253
85. C.Y. Wong, Molecular states of heavy quark mesons. Phys. Rev. C **69**, 055202 (2004). arXiv:hep-ph/0311088
86. E. Braaten, M. Kusunoki, Low-energy universality and the new charmonium resonance at 3870 MeV. Phys. Rev. D **69**, 074005 (2004). arXiv:hep-ph/0311147
87. E.S. Swanson, Short range structure in the $X(3872)$. Phys. Lett. B **588**, 189 (2004). arXiv:hep-ph/0311229
88. Z.Y. Lin, J.B. Cheng, S.L. Zhu, $T_{c\bar{c}}^+$ and $X(3872)$ with the complex scaling method and $DD(\bar{D})\pi$ three-body effect. arXiv:2205.14628 [hep-ph]
89. T.W. Chiu et al., [TWQCD], $X(3872)$ in lattice QCD with exact chiral symmetry. Phys. Lett. B **646**, 95 (2007). arXiv:hep-ph/0603207
90. N. Barnea, J. Vijande, A. Valcarce, Four-quark spectroscopy within the hyperspherical formalism. Phys. Rev. D **73**, 054004 (2006). arXiv:hep-ph/0604010
91. L. Maiani, F. Piccinini, A.D. Polosa, V. Riquer, Diquark-antidiquarks with hidden or open charm and the nature of $X(3872)$. Phys. Rev. D **71**, 014028 (2005). arXiv:hep-ph/0412098
92. H. Hogaasen, J.M. Richard, P. Sorba, A Chromomagnetic mechanism for the $X(3872)$ resonance. Phys. Rev. D **73**, 054013 (2006). arXiv:hep-ph/0511039
93. F.E. Close, S. Godfrey, Charmonium hybrid production in exclusive B meson decays. Phys. Lett. B **574**, 210 (2003). arXiv:hep-ph/0305285

94. B.A. Li, Is $X(3872)$ a possible candidate of hybrid meson. Phys. Lett. B **605**, 306 (2005). arXiv:hep-ph/0410264
95. K.K. Seth, An alternative interpretation of $X(3872)$. Phys. Lett. B **612**, 1 (2005). arXiv:hep-ph/0411122
96. T. Barnes, S. Godfrey, Charmonium options for the $X(3872)$. Phys. Rev. D **69**, 054008 (2004). arXiv:hep-ph/0311162
97. E.J. Eichten, K. Lane, C. Quigg, Charmonium levels near threshold and the narrow state $X(3872) \to \pi^+\pi^- J/\Psi$. Phys. Rev. D **69**, 094019 (2004). arXiv:hep-ph/0401210
98. C. Quigg, The lost tribes of charmonium. Nucl. Phys. Proc. Suppl. **142**, 87 (2005). arXiv:hep-ph/0407124
99. I. Bediaga, J.H. Munoz, Production of radially excited charmonium mesons in two-body nonleptonic B_c decays. arXiv:1102.2190 [hep-ph]
100. L. Nayak, P.C. Dash, S. Kar, N. Barik, Exclusive nonleptonic B_c-meson decays to S-wave charmonium states. Phys. Rev. D **105**, 053007 (2022). arXiv:2202.01167 [hep-ph]
101. J.F. Liu, K.T. Chao, B_c meson weak decays and CP violation. Phys. Rev. D **56**, 4133 (1997)
102. C. Chang, H.F. Fu, G.L. Wang, J.M. Zhang, Some of semileptonic and nonleptonic decays of B_c meson in a Bethe–Salpeter relativistic quark model. Sci. China Phys. Mech. Astron. **58**, 071001 (2015). arXiv:1411.3428 [hep-ph]
103. T. Zhou, T. Wang, H.F. Fu, Z.H. Wang, L. Huo, G.L. Wang, CP violation in non-leptonic B_c decays to excited final states. Eur. Phys. J. C **81**, 339 (2021). arXiv:2012.06135 [hep-ph]
104. Z. Rui, W.F. Wang, G.X. Wang, L.H. Song, C.D. Lu, The $B_c \to \psi(2S)\pi, \eta_c(2S)\pi$ decays in the perturbative QCD approach. Eur. Phys. J. C **75**, 293 (2015). arXiv:1505.02498 [hep-ph]
105. H.W. Ke, X.Q. Li, Z.T. Wei, X. Liu, Re-study on the wave functions of $\Upsilon(nS)$ states in LFQM and the radiative decays of $\Upsilon(nS) \to \eta_b + \gamma$. Phys. Rev. D **82**, 034023 (2010). arXiv:1006.1091 [hep-ph]
106. T. Zhou, T. Wang, Y. Jiang, L. Huo, G.L. Wang, The weak B, B_s and B_c decays to radially excited states. J. Phys. G **48**, 055006 (2021). arXiv:2006.05704 [hep-ph]